

filtration chromatography. This is consistent with the notion that rEhNifS exists as a dimer of two identical subunits (42.5 kDa plus 2.6 kDa corresponding to the histidine tag), which is similar to all other organisms reported earlier. EhNifU was eluted at 150–170 kDa; GST-EhNifU was also eluted at 260–280 kDa (Fig. 7). These results show clearly that EhNifU is a tetramer irrespective of the presence or absence of a fusion partner. Elution patterns of EhNifU remained unchanged when EhNifU was pretreated with 2 mM DTT and fractionated in the presence of DTT (results not shown).

Anion-Exchange Chromatographic Separation of Native and Recombinant Cysteine Desulfurase Activity—To correlate native cysteine desulfurase activity in the *E. histolytica* lysate with the recombinant enzyme, the lysate from the trophozoites and rEhNifS were subjected to chromatographic separation on a Mono Q anion exchange column and analyzed by cysteine desulfurase assay and also immunoblotting using anti-EhCS, EhMGL, and EhNifS antibodies. *E. histolytica* trophozoites possess two isotypes of CS (CS1 and CS2) (41) and two isotypes of MGL (MGL1 and MGL2) (46), both of which showed substantial cysteine desulfurase activity.⁶ Thus, we attempted to separate native NifS from the CS and MGL isotypes. The *E. histolytica* lysate showed three major peaks of cysteine desulfurase activity (Fig. 8A). Fractions corresponding to the last and largest cysteine desulfurase peak (fractions 20–27) contained the protein that reacted well with the anti-EhNifS and anti-CS antibodies (Fig. 8B). In contrast, fractions corresponding to the first and second cysteine desulfurase peaks did not react with anti-EhNifS antibody but reacted with anti-MGL and anti-CS antibodies, respectively. rEhNifS was fractionated under the same conditions and showed a single peak eluted at a slightly lower ionic strength (0.5 ml earlier elution volume) than the native EhNifS (Fig. 8C), which is consistent with the fact that recombinant histidine-tagged EhNifS has a slightly higher pI (6.15) than the native protein (5.9). These results suggest that the third dominant cysteine desulfurase peak of the parasite lysate represents activity mainly attributable to native EhNifS.

Heterologous Expression of the Amebic NifS and NifU in the *isc/suf*-Mutant *E. coli* Strain—To assess the *in vivo* role of EhNifS and EhNifU, we attempted heterologous complementation of an *E. coli* mutant UT109 in which the chromosomal *isc* and *suf* operons were deleted. This strain was lethal unless we provided the *suf* or *isc* operon in a complementing plasmid carrying a temperature-sensitive replicative origin.⁷ At the restrictive temperature, introduction of the *E. coli* *isc* or *suf* operon in a complementing plasmid carrying a temperature-insensitive replicative origin complemented the growth defects of the UT109 strain under both the aerobic and anaerobic conditions (Fig. 9). In contrast, coexpression of EhNifS and EhNifU rescued the growth of UT109 only under the anaerobic, not aerobic, conditions at the restrictive temperature. Thus, the amebic NifS and NifU are apparently necessary and sufficient for the Fe-S cluster formation under anaerobic conditions in this heterologous system. Although CS and MGL showed cysteine desulfurase activity *in vitro*, coexpression of CS1 or MGL2, together with EhNifU, did not complement the growth defects of UT109 under either aerobic or anaerobic conditions (data not shown).

DISCUSSION

We have identified and characterized two necessary and sufficient components, NifS and NifU, of the NIF-like system for the assembly of Fe-S clusters in a human intestinal proto-

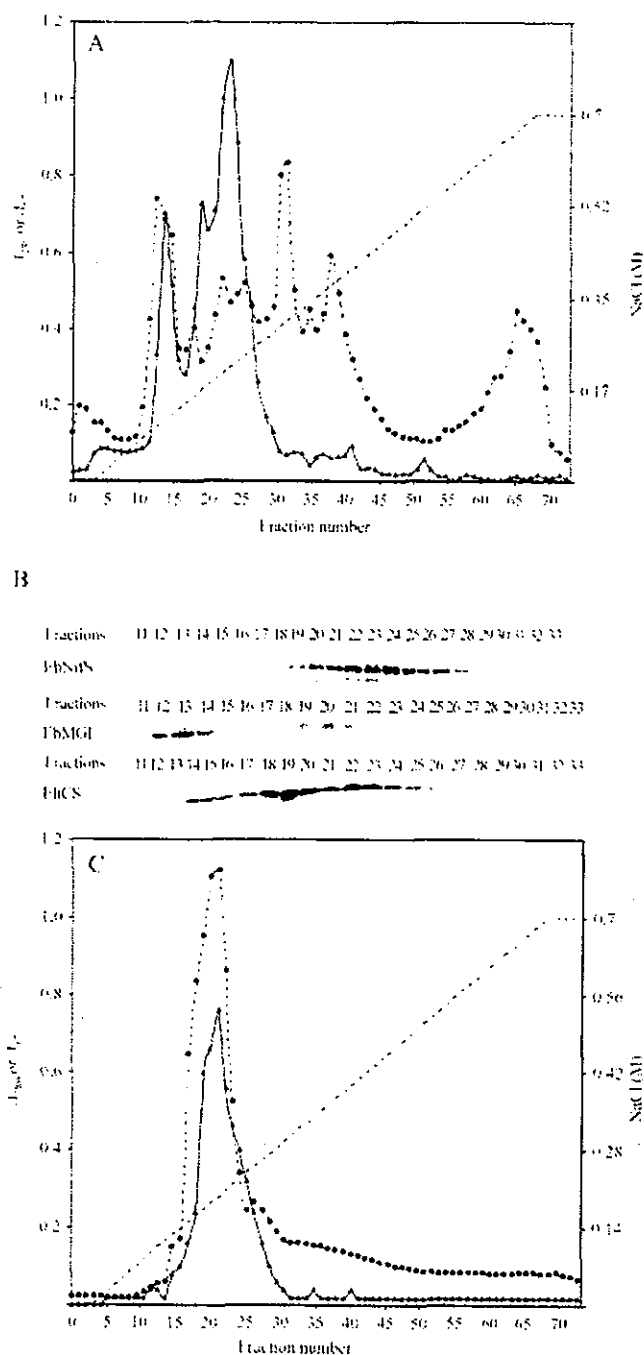


Fig. 8. Separation of the native EhNifS from the *E. histolytica* trophozoites and rEhNifS with Mono Q anion exchange chromatography. A, elution profile of the native EhNifS. The total lysate of *E. histolytica* trophozoites was separated on the anion exchange column at pH 8.0 with a linear gradient of NaCl (dashed line) (0–0.7 M). Triangles and an unbroken line depict cysteine desulfurase activity, shown as A_{670} . Circles and a broken line show A_{280} . B, immunoblots of each fraction with anti-EhNifS, MGL, and CS antibodies. C, elution profile of the recombinant EhNifS. The rEhNifS protein was fractionated under the same conditions as in A. Triangles and an unbroken line show cysteine desulfurase activity. Circles and a broken line represent A_{280} . A dashed line represents NaCl concentrations of a linear gradient.

zoan anaerobe. As far as we are aware, this is the first demonstration of the NIF-like system in eukaryotes. Despite a thorough search of the *E. histolytica* genome database, no other proteins that were shown to be involved in ISC/SUF systems of other organisms were found, suggesting that this parasite possesses the NIF-like system as a sole and non-redundant system for the biosynthesis of all Fe-S proteins. Because *E. histolytica*

⁶ V. Ali and T. Nozaki, unpublished data.

⁷ U. Tokumoto and Y. Takahashi, manuscript in preparation.

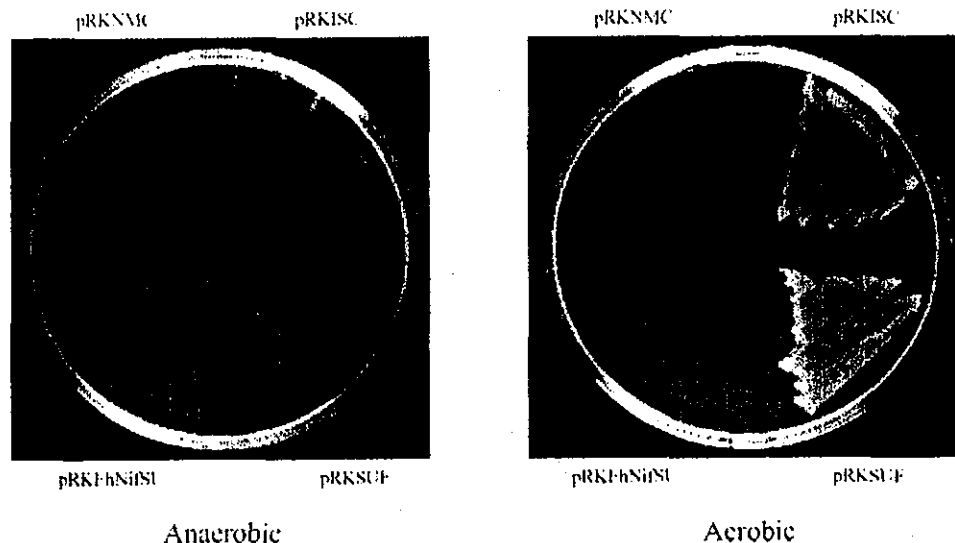


FIG. 9. Functional complementation of the *isc/suf*-mutant *E. coli* strain by coexpression of EhNifS and EhNifU under anaerobic conditions. pRKEhNifSU, pRKISC, or pRKSUF, which contains *E. histolytica* EhNifS and EhNifU, *E. coli iscSUA-hscBA-fox*, or *E. coli sufABCDSE* operon, respectively, in pRKNMC, or pRKNMC alone was introduced into *E. coli* strain UT109 [$\Delta(iscSUA-hscBA)::Km^r$, $\Delta(sufABCDSEU)::Gm^r$] as described in "Experimental Procedures." The transformants were cultivated at the restrictive temperature under either aerobic or anaerobic conditions.

does not possess nitrogenase and is incapable of nitrogen fixation, the presence of the NIF-like system and the lack of other systems in this organism reinforce the premise that the NIF system is not specific for the Fe-S cluster formation of nitrogenase but is involved in the Fe-S cluster assembly for nitrogenase and non-nitrogenase proteins, as proposed for the NIF-like system in *H. pylori* (13). Our *in vivo* complementation of a temperature-dependent growth defect of the *E. coli isc/suf* mutant strain by expression of a heterologous NIF-like system indicates that the NIF-like system plays an interchangeable role in the Fe-S cluster assembly of non-nitrogenase proteins with the ISC or SUF system under anaerobic conditions. Despite common catalytic and scaffold mechanisms shared by the NIF, ISC, and SUF systems, there are a number of differences among these systems (10); the ISC and SUF systems appear to be considerably more complex than the NIF system. For example, heat-shock-cognate (Hsc) proteins have been suggested to have chaperone-like functions in the ISC system for the formation of transient Fe-S clusters or insertion into various target proteins in bacteria and yeast (7, 26, 30, 50, 51). Our *in vivo* complementation study revealed that the NIF-like system does not require any additional component other than NifS and NifU for Fe-S cluster assembly under anaerobic conditions. However, it is also possible that as yet unidentified proteins that remain in the *isc/suf*-mutant strain of *E. coli* function together with the exogenous NifS and NifU. It is also conceivable that the NIF-like system is shared by other anaerobic parasitic organisms. However, two other well-characterized anaerobic protozoan parasites *G. lamblia* and *T. vaginalis* appear to possess the ISC and lack the NIF system (32, 34). Thus, the presence of the NIF-like system is likely unique to *E. histolytica*, which might be attributable to a rare horizontal gene transfer from a NIF-like-containing prokaryotic organism (see below).

Several lines of evidence support close kinship between the amebic NifS and NifU and their homologs from ϵ -proteobacteria. First, phylogenetic analyses indicate that *E. histolytica* and ϵ -proteobacteria represent an independent clade well separated from other NifS and NifU homologs. Second, this close phylogenetic association is also supported by the common insertions and deletions of amino acids shared by NifS and NifU from these organisms. Third, the multimeric structure of the

amebic and *H. pylori* NifU is identical (*i.e.* tetramer), whereas NifU from *A. vinelandii* and IscU from *E. coli* and yeast form a dimer. Fourth, UV/visible absorption spectra and specific activity of EhNifS were comparable to the *H. pylori* NifS but notably different from *A. vinelandii*. These data suggest that amebic *nif*-like genes were likely obtained from an ancestral organism currently represented by ϵ -proteobacteria by lateral gene transfer, as suggested for other metabolic enzymes that are proposed to have been transferred from Archaea and/or bacteria by a similar mechanism (52–54).

Fractionation of the crude extract of *E. histolytica* by anion-exchange chromatography revealed that at least three groups of enzymes, CS, MGL, and NifS, contributed to cysteine desulfurase activity, *i.e.* activity to mobilize the sulfur or sulfide from L-cysteine, and thus possibly provide sulfur for Fe-S cluster synthesis. Although both CS and MGL showed cysteine desulfurase activity⁶ (see also "Results" and Ref. 16 for *E. coli* CS) and also *in vitro* activity to convert an apo form of recombinant amebic [4Fe-4S]²⁺ ferredoxin (53, 55) into a holo form,⁶ we argue that EhNifS is the sole protein that functions in Fe-S cluster biosynthesis *in vivo*. Expression of CS or MGL (*i.e.* EhCS1 or EhMGL2), when coexpressed with EhNifU, did not complement the Fe-S cluster formation of the *isc/suf*-mutant strain of *E. coli* (data not shown). This reinforces the previous observation on *E. coli* cysteine synthase A, B, and γ -cystathionase (16) and indicates that the *in vitro* conversion assay of apo Fe-S protein does not reflect *in vivo* function.

We did not demonstrate in the present study the species of the temporal Fe-S cluster (*i.e.* [2Fe-2S]²⁺ or [4Fe-4S]²⁺) that formed on EhNifU in addition to the stable [2Fe-2S]²⁺ cluster shown in Fig. 6. However, it is conceivable, by analogy to NifU from *A. vinelandii* involved in the Fe-S cluster formation of nitrogenase, that amebic NifU functions as an intermediate site for the transient [2Fe-2S]²⁺ cluster assembly (12). The putative labile [2Fe-2S]²⁺, if present, was likely lost during purification under aerobic conditions. We also speculate that the transition of Fe-S clusters on EhNifU may occur under anaerobic conditions; one [4Fe-4S]²⁺ cluster may be formed from two [2Fe-2S]²⁺ clusters, as shown for *Azotobacter* IscU (5). Because the amebic NifU forms a tetramer, the mechanism of the [4Fe-4S]²⁺ cluster formation from [2Fe-2S]²⁺ on NifU may differ from *Azotobacter* NifU, which exists as a dimer. Because

E. histolytica is not a nitrogen-fixing organism, the NIF-like system is not necessarily specific for nitrogenase proteins, but they are also involved in Fe-S cluster assembly for other Fe-S proteins, as shown previously for *H. pylori* (13). Although all characterized or putative Fe-S proteins in the genome database of *E. histolytica*, including ferredoxins and pyruvate:ferredoxin oxidoreductase, likely contain $2[4\text{Fe-4S}]^{2+}$ clusters, the fact that the amebic NIF-like system functions in the formation of the $[2\text{Fe-2S}]^{2+}$ cluster in *E. coli* indicates that the amebic NIF-like system is involved in the biosynthesis of all forms of Fe-S clusters.

Acknowledgments—We are grateful to Toshiharu Hase, Institute for Protein Research, Osaka University, and Kiyoshi Kita, University of Tokyo, Japan for valuable discussions.

REFERENCES

- Beinert, H., Holm, R. H., and Munck, E. (1997) *Science* **277**, 653–659
- Zheng, L., White, R. H., Cash, V. L., Jack, R. F., and Dean, D. R. (1993) *Proc. Natl. Acad. Sci. U. S. A.* **90**, 2754–2758
- Zheng, L., White, R. H., Cash, V. L., and Dean, D. R. (1994) *Biochemistry* **33**, 4714–4720
- Zheng, L., Cash, V. L., Flint, D. H., and Dean, D. R. (1998) *J. Biol. Chem.* **273**, 13264–13272
- Agar, J. N., Krabs, C., Frazzon, J., Huynh, B. H., Dean, D. R., and Johnson, M. K. (2000) *Biochemistry* **39**, 7856–7862
- Tokumoto, U., and Takahashi, Y. (2001) *J. Biochem. (Tokyo)* **130**, 63–71
- Takahashi, Y., and Nakamura, M. (1999) *J. Biochem. (Tokyo)* **126**, 917–926
- Takahashi, Y., and Tokumoto, U. (2002) *J. Biol. Chem.* **277**, 28380–28383
- Kaiser, J. T., Clausen, T., Bourenkova, G. P., Bartunik, H. D., Steinbacher, S., and Huber, R. (2000) *J. Mol. Biol.* **297**, 451–464
- Yuvaniyama, P., Agar, J. N., Cash, V. L., Johnson, M. K., and Dean, D. R. (2000) *Proc. Natl. Acad. Sci. U. S. A.* **97**, 599–604
- Fu, W., Jack, R. F., Morgan, T. V., Dean, D. R., and Johnson, M. K. (1994) *Biochemistry* **33**, 13455–13463
- Agar, J. N., Yuvaniyama, P., Jack, R. F., Cash, V. L., Smith, A. D., Dean, D. R., and Johnson, M. K. (2000) *J. Biol. Inorg. Chem.* **5**, 167–177
- Olson, J. W., Agar, J. N., Johnson, M. K., and Maier, R. J. (2000) *Biochemistry* **39**, 16213–16219
- Schwartz, C. J., Djaman, O., Imlay, J. A., and Kiley, P. J. (2000) *Proc. Natl. Acad. Sci. U. S. A.* **97**, 9009–9014
- Kato, S., Mihara, H., Kurihara, T., Takahashi, Y., Tokumoto, U., Yoshimura, T., and Esaki, N. (2002) *Proc. Natl. Acad. Sci. U. S. A.* **99**, 5948–5952
- Flint, D. H. (1996) *J. Biol. Chem.* **271**, 16068–16074
- Wu, G., Mansy, S. S., Hemann, C., Hille, R., Surer, K. K., and Cowan, J. A. (2002) *J. Biol. Inorg. Chem.* **7**, 526–532
- Ollagnier-de-Choudens, S., Mattioli, T., Takahashi, Y., and Fontecave, M. (2001) *J. Biol. Chem.* **276**, 22604–22607
- Hoff, K. G., Silberg, J. J., and Vickery, L. E. (2000) *Proc. Natl. Acad. Sci. U. S. A.* **97**, 7790–7795
- Tokumoto, U., Nomura, S., Minami, Y., Mihara, E., Shin-ichiro, K., Kurihara, T., Esaki, N., Kanazawa, H., Matsubara, H., and Takahashi, Y. (2002) *J. Biochem. (Tokyo)* **131**, 713–719
- Nachin, L., EL Hassouni, M., Loiseau, L., Expert, D., and Barras, F. (2001) *Mol. Microbiol.* **39**, 960–972
- Zheng, M., Wang, X., Templeton, L. J., Smulski, D. R., LaRossa, R. A., and Storz, G. (2001) *J. Bacteriol.* **183**, 4562–4570
- Patzer, S. I., and Hantke, K. (1999) *J. Bacteriol.* **181**, 3307–3307
- Nachin, L., Loiseau, L., Expert, D., and Barras, F. (2003) *EMBO J.* **22**, 427–437
- Loiseau, L., Ollagnier-de-Choudens, S., Nachin, L., Fontecave, M., and Barras, F. (2003) *J. Biol. Chem.* **278**, 38352–38359
- Strain, J., Lorenz, C. R., Bode, J., Garland, S., Smolen, G. A., Ta, D. T., Vickery, L. E., and Culotta, V. C. (1998) *J. Biol. Chem.* **273**, 31138–31144
- Nakai, Y., Yoshihara, Y., Hayashi, H., and Kagamiyama, H. (1998) *FEBS Lett.* **433**, 143–148
- Schilke, B., Voisine, C., Beinert, H., and Craig, E. (1999) *Proc. Natl. Acad. Sci. U. S. A.* **96**, 10206–10211
- Tong, W. H., Jameson, G. N. L., Huynh, B. H., and Rouault, T. A. (2003) *Proc. Natl. Acad. Sci. U. S. A.* **100**, 9762–9767
- Kispal, G., Csere, P., Prohl, C., and Lill, R. (1999) *EMBO J.* **18**, 3981–3989
- Tong, W. H., and Rouault, T. (2000) *EMBO J.* **19**, 5692–5700
- Muhlenhoff, U., and Lill, R. (2000) *Biochim. Biophys. Acta* **1459**, 370–382
- Ellis, K. E. S., Clough, B., Saldanha, J. W., and Wilson, R. J. M. (2001) *Mol. Microbiol.* **41**, 973–981
- Tachezy, J., Sanchez, L. B., and Muller, M. (2001) *Mol. Biol. Evol.* **18**, 1919–1928
- Martin, W., and Muller, M. (1998) *Nature* **392**, 37–41
- Tovar, J., Leon-Avila, G., Sanchez, L. B., Sutak, R., Tachezy, J., Van Der Giezen, M., Hernandez, M., Muller, M., and Luccocq, J. M. (2003) *Nature* **426**, 172–176
- Diamond, L. S., Mattern, C. F., and Bartgis, I. L. (1972) *J. Virol.* **9**, 326–341
- Diamond, L. S., Harlow, D. R., and Cunnick, C. C. (1978) *Trans. R. Soc. Trop. Med. Hyg.* **72**, 431–432
- Thompson, J. D., Higgins, D. G., and Gibson, T. J. (1994) *Nucleic Acids Res.* **22**, 4673–4680
- Page, R. D. (1996) *Comput. Appl. Biosci.* **12**, 357–358
- Nozaki, T., Asai, T., Kobayashi, S., Ikegami, F., Noji, M., Saito, K., and Takeuchi, T. (1998) *Mol. Biochem. Parasitol.* **97**, 33–44
- Jaschkowitz, K., and Seidler, A. (2000) *Biochemistry* **39**, 3416–3423
- Siegel, L. M. (1965) *Anal. Biochem.* **11**, 126–132
- Wood, J. L. (1987) *Methods Enzymol.* **143**, 25–29
- Sambrook, J., Fritsch, E. F., and Maniatis, T. (2001) *Molecular Cloning: A Laboratory Manual*, 3rd Ed., Cold Spring Harbor Laboratory Press, Cold Spring Harbor, NY
- Tokoro, M., Asai, T., Kobayashi, S., Takeuchi, T., and Nozaki, T. (2003) *J. Biol. Chem.* **278**, 42717–42727
- Garland, S. A., Hoff, K., Vickery, L. E., and Culotta, V. C. (1999) *J. Mol. Biol.* **294**, 897–907
- Mihara, H., Kurihara, T., Yoshimura, T., Soda, K., and Esaki, N. (1997) *J. Biol. Chem.* **272**, 22417–22424
- Benci, S., Vaccari, S., Mozzarelli, A., and Cook, P. F. (1999) *Biochim. Biophys. Acta* **1429**, 317–330
- Sellers, V. M., Wang, K. F., Johnson, M. K., and Dailey, H. A. (1998) *J. Biol. Chem.* **273**, 22311–22316
- Silberg, J. J., Hoff, K. G., and Vickery, L. E. (1998) *J. Bacteriol.* **180**, 6617–6624
- Field, J., Rosenthal, B., and Samuelson, J. (2000) *Mol. Microbiol.* **38**, 446–455
- Nixon, J. E., Wang, A., Field, J., Morrison, H. G., McArthur, A. G., Sogin, M. L., Loftus, B. J., and Samuelson, J. (2002) *Eukaryot. Cell* **1**, 181–190
- Ali, V., Shigeta, Y., and Nozaki, T. (2003) *Biochem. J.* **375**, 729–736
- Reeves, R. E., Guthrie, J. D., and Lobelle-Rich, P. (1980) *Exp. Parasitol.* **49**, 83–88

Molecular and biochemical characterization of D-phosphoglycerate dehydrogenase from *Entamoeba histolytica*

A unique enteric protozoan parasite that possesses both phosphorylated and nonphosphorylated serine metabolic pathways

Vahab Ali¹, Tetsuo Hashimoto², Yasuo Shigeta¹ and Tomoyoshi Nozaki^{1,3}

¹Department of Parasitology, National Institute of Infectious Diseases, Tokyo, Japan; ²Institute of Biological Sciences, University of Tsukuba, Japan; ³Precursory Research for Embryonic Science and Technology, Japan Science and Technology Agency, Tokyo, Japan

A putative phosphoglycerate dehydrogenase (PGDH), which catalyzes the oxidation of D-phosphoglycerate to 3-phosphohydroxypyruvate in the so-called phosphorylated serine metabolic pathway, from the enteric protozoan parasite *Entamoeba histolytica* was characterized. The *E. histolytica* PGDH gene (*EhPGDH*) encodes a protein of 299 amino acids with a calculated molecular mass of 33.5 kDa and an isoelectric point of 8.11. EhPGDH showed high homology to PGDH from bacteroides and another enteric protozoan ciliate, *Entodinium caudatum*. EhPGDH lacks both the carboxyl-terminal serine binding domain and the 13–14 amino acid regions containing the conserved Trp139 (of *Escherichia coli* PGDH) in the nucleotide binding domain shown to be crucial for tetramerization, which are present in other organisms including higher eukaryotes. EhPGDH catalyzed reduction of phosphohydroxypyruvate to phosphoglycerate utilizing NADH and, less efficiently, NADPH; EhPGDH did not utilize 2-oxoglutarate. Kinetic parameters of EhPGDH were similar to those of mamma-

lian PGDH, for example the preference of NADH cofactor, substrate specificities and salt-reversible substrate inhibition. In contrast to PGDH from bacteria, plants and mammals, the EhPGDH protein is present as a homodimer as demonstrated by gel filtration chromatography. The *E. histolytica* lysate contained PGDH activity of 26 nmol NADH utilized per min per mg of lysate protein in the reverse direction, which consisted 0.2–0.4% of a total soluble protein. Altogether, this parasite represents a unique unicellular protist that possesses both phosphorylated and nonphosphorylated serine metabolic pathways, reinforcing the biological importance of serine metabolism in this organism. Amino acid sequence comparison and phylogenetic analysis of various PGDH sequences showed that *E. histolytica* forms a highly supported monophyletic group with another enteric protozoa, ciliate *E. caudatum*, and bacteroides.

Keywords: anaerobic protist; cysteine biosynthesis; serine biosynthesis.

L-Serine is a key intermediate in a number of important metabolic pathways. In addition to its role in the synthesis of L-cysteine and L-glycine and also in the formation of L-methionine by the interconversion of L-cysteine via

L-cystathionine, L-serine is a major precursor of phosphatidyl-L-serine, sphingolipids, taurine, porphyrins, purines, thymidine and neuromodulators D-serine and D-glycine [1,2]. L-Serine is synthesized from a glycolytic intermediate 3-phosphoglycerate (3-PGA) in the so-called phosphorylated serine pathway in mammals. In plants, two pathways have been shown to be involved in serine biosynthesis: the phosphorylated pathway, which functions in plastids of nonphotosynthetic tissues and also under dark conditions [3], and the glycolate pathway, which is present in mitochondria of photosynthetic tissues and functions under light conditions [4,5]. D-Phosphoglycerate dehydrogenase (PGDH, EC 1.1.1.95) catalyses the NAD⁺- or NADP⁺-linked oxidation of 3-PGA in the first step of the phosphorylated serine biosynthetic pathway [6]. The PGDH activity from *Escherichia coli* [7], *Bacillus subtilis* [8], and pea [9] was shown to be subjected to allosteric control by the end product of the pathway, serine. However, such allosteric inhibition was not demonstrated for PGDH from other plants [3,10] and animals [11–13]. Substrate inhibition of the PGDH activity by 3-phosphohydroxypyruvate (PHP) at > 10 μM, which was reversed by high concentrations of salts, in the reverse (nonphysiological) direction, was also observed for PGDH from rat liver [13], but not for PGDH

Correspondence to T. Nozaki, Department of Parasitology, National Institute of Infectious Diseases, 1-23-1 Toyama, Shinjuku-ku, Tokyo 162-8640, Japan. Fax: + 81 3 5285 1173, Tel.: + 81 3 5285 1111 ext. 2733, E-mail: nozaki@nih.go.jp

Abbreviations: PHP, phosphohydroxypyruvate; 3-PGA, 3-phosphoglyceric acid; PGDH, D-phosphoglycerate dehydrogenase; GDH, D-glycerate dehydrogenase; PSAT, phosphoserine aminotransferase; EhPGDH, *Entamoeba histolytica* D-phosphoglycerate dehydrogenase; ML, maximum likelihood; NJ, neighbor joining; MP, maximum parsimony; BP, bootstrap proportion.

Enzymes: D-3-phosphoglycerate dehydrogenase (EC 1.1.1.95); D-glycerate dehydrogenase (EC 1.1.1.29); phosphoserine aminotransferase (EC 2.6.1.52); D-glycerate kinase (EC 2.7.1.31).

Note: The nucleotide sequence data of *E. histolytica* PGDH reported in this paper has been submitted to the DDBJ/GenBank/EBI data bank with Accession number AB091512.

(Received 12 February 2004, revised 27 April 2004, accepted 30 April 2004)

from bacteria [8] and plants [9]. Thus, the presence or absence of allosteric and substrate inhibition of this enzyme appears to be organism specific.

PGDH from rat liver was shown to be upregulated at the transcriptional level with protein-poor and carbohydrate-rich diet [14]. Previous enzymological studies using both native [7–9,15] and recombinant [3,13,16,17] PGDH from bacteria, plants and mammals showed that PGDH forms a homotetramer with a monomer molecular mass of 44–67 kDa. Each 44 kDa subunit of the homotetrameric PGDH from *E. coli* has three distinct domains: the nucleotide binding domain (residues 108–294), the substrate binding domains (residues 7–107 and 295–336) and the regulatory domain (residues 337–410), the latter of which binds to L-serine [18]. The major protein–protein interactions between the subunits have been implicated at the nucleotide binding domains and the regulatory domain, indicating the importance of these domains for the tetramerization of the enzyme [18]. It was shown that serine binding induces a conformational change at the regulatory domain interfaces of PGDH, and serine is subsequently transferred to the active site to elicit inhibition of catalysis [19,20]. The PGDH activity was inhibited by approximately 90% when two of the four serine binding sites of the PGDH tetramer were bound to serine [19], indicating that the binding of a single serine at each of the two regulatory site interfaces is sufficient to affect all four active sites. Physiological importance of PGDH in serine biosynthesis has been demonstrated in its deficiency in human [12,21]. Patients with PGDH deficiency exhibit a marked decrease of L-serine and glycine concentrations in both plasma and cerebrospinal fluid [12,21–23], which results in severe neurological disorders, i.e. congenital microcephaly, dysmyelination, intractable seizures, and psychomotor retardation.

Entamoeba histolytica is the enteric protozoan parasite that causes amoebic colitis and extra intestinal abscesses (e.g. hepatic, pulmonary and cerebral) in approximately 50 million inhabitants of endemic areas [24]. Among a number of metabolic peculiarities, metabolism of sulfur-containing amino acids in *E. histolytica* has been shown to be unique in a variety of aspects including: (a) a lack of both forward and reverse transsulfuration pathways [25], (b) the presence of a unique enzyme methionine γ -lyase involved in the degradation of sulfur-containing amino acids [25] and (c) the presence of *de novo* sulfur-assimilatory cysteine biosynthetic pathway [26,27]. The physiological importance of cysteine has previously been shown for this parasite. Cysteine plays an essential role in survival, growth and attachment of parasite [28,29], and also in antioxidative defense mechanism [27]. As the major, if not sole, route of cysteine biosynthesis in this parasite is the condensation of *O*-acetylserine with sulfide by the *de novo* cysteine biosynthetic pathway, molecular identification of enzymes and their genes located upstream of this pathway is essential. We attempted to identify and characterize the putative serine metabolic pathway (a general scheme for serine biosynthetic and degradative pathways is shown in Fig. 1). We previously identified, in the *E. histolytica* genome database, genes encoding PGDH (EC 1.1.1.95), glycerate kinase (GK, EC 2.7.1.31), phosphoserine aminotransferase (PSAT, EC 2.6.1.52), and D-glycerate dehydrogenase (GDH,

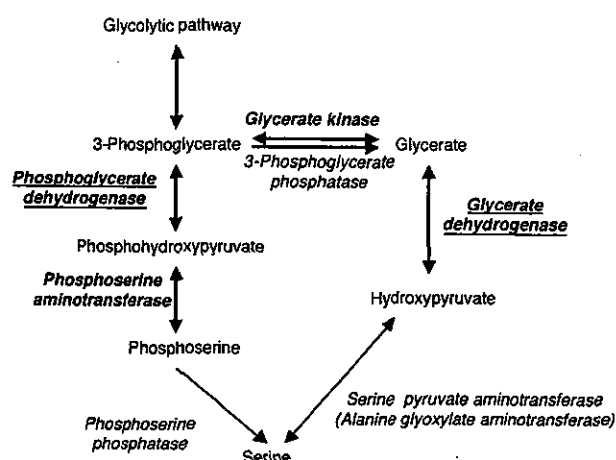


Fig. 1. A general scheme of serine metabolism. Enzymes identified in the *E. histolytica* genome database are shown in bold. Enzymes previously characterized [30] or reported in the present work are also underlined.

EC 1.1.1.29) [30], suggesting that this parasite possesses both phosphorylated and nonphosphorylated pathways. We showed that GDH probably plays a role in serine degradation, rather than biosynthesis and, thus, in the down-regulation of the intracellular serine concentration [30].

In the present work, we describe cloning and enzymological characterization of native and recombinant amoebic PGDH. This is the first report on PGDH from unicellular eukaryotes. The amoebic PGDH represents a new member of PGDH, which is supported by amino acid sequence comparisons and phylogenetic studies. The amoebic PGDH (a) lacks the carboxyl-terminal serine binding regulatory domain, which is implicated for allosteric inhibition and tetramerization, and the essential Trp residue in the nucleotide binding domain, inferred also for tetramerization, and (b) exists as a homodimer, dissimilar to PGDH from other organisms.

Materials and methods

Chemicals

All chemicals of analytical grade were purchased from Wako (Tokyo, Japan) unless otherwise stated. Hydroxy-pyruvic acid phosphate dimethylketal (cyclohexylammonium) salt, D-phosphoglyceric acid, NADPH, NADH, NAD⁺ and NADP⁺ were purchased from Sigma-Aldrich (Tokyo, Japan). PHP was prepared from the hydroxy-pyruvic acid phosphate dimethylketal (cyclohexylammonium) salt as described previously [31]. Pre-packed Mono Q 5/5 HR and Sephacryl S 300 Hiprep columns were purchased from Amersham Biosciences (Tokyo, Japan).

Parasite cultivation

Trophozoites of the pathogenic *E. histolytica* clonal strain HM1:IMSS cl 6 [32] were axenically cultured in BI-S-33 medium at 35 °C as described previously [33].

Expression and purification of recombinant *E. histolytica* PGDH (rEhPGDH)

A plasmid was constructed to produce rEhPGDH with the amino-terminal histidine tag. A fragment corresponding to an open reading frame (ORF) of EhPGDH was amplified by PCR using a cDNA library [26] as a template, and oligonucleotide primers (5'-caGGATCCAagatagttgtgataac cga-3' and 5'-caCTCGAGTtagaactattgactggaa-3'), where capital letters indicate the *Bam*HI or *Xho*I restriction sites. The PCR was performed with the following parameters: (a) an initial incubation at 95 °C for 5 min; (b) 30 cycles of denaturation at 94 °C for 30 s, annealing at 55 °C for 30 s, and elongation at 72 °C for 1 min; and (c) a final extension at 72 °C for 10 min. The ≈ 1.0 kb PCR fragment was digested with *Bam*HI and *Xho*I, electrophoresed, purified with GeneClean kit II (BIO 101, Vista, CA), and cloned into *Bam*HI- and *Xho*I-double-digested pET-15b (Novagen, Darmstadt, Germany) in the same orientation as the T7 promoter to produce pET-EhPGDH. The nucleotide sequence of the amplified EhPGDH ORF was verified by sequencing and found to be identical to a putative protein coding region of EH01468 (contig 318390, nucleotides 31494–32394) in the *E. histolytica* genome database available at The Institute for Genomic Researches (TIGR) (<http://www.tigr.org>). The pET-EhPGDH construct was introduced into the *E. coli* BL21 (DE3) cell (Novagen). Expression of the rEhPGDH protein was induced with 0.4 mM isopropyl thio-β-D-galactoside for 4–5 h at 30 °C. The bacterial cells were harvested, washed with phosphate-buffered saline (NaCl/P_i), pH 7.4, resuspended in the lysis buffer (50 mM Tris/HCl, 300 mM NaCl, pH 8.0, and 10 mM imidazole) containing 0.1% (v/v) Triton X-100, 100 μg mL⁻¹ lysozyme and Complete Mini EDTA free protease inhibitor cocktail (Roche, Tokyo, Japan), sonicated, and centrifuged at 24 000 g at 4 °C for 15 min. The histidine-tagged rEhPGDH protein was purified from the supernatant fraction using a nickel-nitrilotriacetic acid column (Novagen) as instructed by the manufacturer. After the supernatant fraction was mixed and incubated with nickel-nitrilotriacetic acid agarose at 4 °C for 1 h, the agarose was washed with a series of washing buffer (20 mM Tris/HCl, 300 mM NaCl, pH 8.0 containing 10, 20, 35 or 50 mM imidazole). The histidine-tagged rEhPGDH protein was eluted with 100 mM imidazole and extensively dialyzed in 50 mM Tris/HCl, 300 mM NaCl (pH 8.0) containing 10% (v/v) glycerol and the protease inhibitors as described above, overnight at 4 °C. The dialyzed protein was stored at –80 °C with 50% (v/v) glycerol in small aliquots until use. The purified rEhPGDH remained active for more than one month when stored at –80 °C.

Enzyme assays

3-PGA-dependent production of NADH in the forward direction was measured fluorometrically using a Fluorometer (F-2500, Hitachi, Tokyo, Japan), with an activation at 340 nm and an emission at 470 nm, for 2–4 min at 25 °C. Because the forward reaction showed an optimum pH of 9.0, all reactions were carried out at this pH. The assay mixture contained 100 mM Tris/HCl,

pH 9.0, 400 mM NaCl, 0.2 mM NAD⁺, 0.2 mM dithiothreitol, 3.0 mM 3-PGA and 1.6 μg of the rEhPGDH or appropriate amounts of fractions of the parasite lysate, in 300 μL of reaction mixture. The kinetic parameters were determined by using variable concentration of 3-PGA (50 μM to 10 mM), NADP⁺ (50 μM to 0.4 mM) and NAD⁺ (5.0 μM to 0.3 mM). The reaction was initiated by the addition of 3-PGA. The PGDH activity in the reverse reaction was measured both fluorometrically and spectrophotometrically. The reaction mixture contained 50 mM NaCl/P_i, pH 6.5, 400 mM NaCl, 0.2 mM NADH or NADPH, 0.2 mM dithiothreitol, 100 μM PHP and 1.2 μg of rEhPGDH or appropriate amounts of fractions of the parasite lysate in 300 μL. The kinetic parameters for reversed reaction were determined by using variable amount of PHP (5–500 μM) and NADH (1–300 μM). The enzymatic activities were expressed in units/mg protein⁻¹. One unit was defined as the amount of enzyme that catalyses the utilization or production of 1.0 μmol of NADH per min under the conditions mentioned above. *K*_m and *V*_{max} were estimated with Lineweaver–Burk and Hanes–Woolf plots.

Chromatographic separation of EhPGDH from *E. histolytica* lysate

Approximately 10⁷ *E. histolytica* trophozoites were washed twice with ice-cold NaCl/P_i. After centrifugation at 500 g for 5 min, the cell pellet (150–200 mg) was resuspended in 1.0 mL of 100 mM Tris/HCl, pH 9.0, 1.0 mM EDTA, 2.0 mM dithiothreitol and 15% (v/v) glycerol containing 10 μg mL⁻¹ *trans*-epoxysuccinyl-L-leucylamido-(4-guanidino)butane (E64) and Complete Mini EDTA-free protease inhibitor cocktail. The cell suspension was then subjected to three cycles of freezing and thawing. After the suspension was further sonicated, the crude lysate was centrifuged at 45 000 g for 15 min at 4 °C and filtered through a 0.45 μm cellulose acetate membrane. The sample was applied to Mono Q 5/5 HR column pre-equilibrated with the binding buffer [100 mM Tris/HCl, pH 9.0, 1.0 mM EDTA, 2.0 mM dithiothreitol, 15% (v/v) glycerol and 1 μg mL⁻¹ E64] on AKTA Explorer 10S system (Amersham Biosciences). After the column was extensively washed with the binding buffer, bound proteins were eluted with a linear gradient of 0–1 M NaCl. Each fraction (0.5 mL) was analyzed for PGDH activity by monitoring the decrease in the absorbance at 340 nm spectrophotometrically as described above. The rEhPGDH was dialyzed against the binding buffer and also fractionated on the same column under the identical condition. An apparent molecular mass of the recombinant EhPGDH was determined by gel filtration chromatography using Sephacryl S300 HR Hiprep prepacked column (60 cm long and 1.6 cm in diameter). The column was pre-equilibrated, washed and eluted with the gel filtration buffer (0.1 M Tris/HCl, pH 8.0 and 0.1 M NaCl) with a flow rate of 0.5 mL min⁻¹. An apparent molecular mass of the EhPGDH monomer was also determined by SDS/PAGE under denaturing conditions as described previously [34].

Amino acid sequence comparison and phylogenetic analysis

All sequence data, except the *E. histolytica* PGDH originally reported in this work, were collected from public databases, including genome sequencing project databases. Multiple alignments for 35 PGDH and eight GDH sequences were accomplished by the CLUSTAL W program version 1.81 [35] with BLOSUM 62 matrix. We included GDH sequences as we assumed that they are biochemically paralogous to PGDH sequences and represent the closest member of the 2-hydroxyacid dehydrogenase family. In addition, the GDH sequence was also available from *E. histolytica* [30]. The alignment obtained was corrected by manual inspection, and unambiguously aligned 182 sites were selected and used for phylogenetic analysis. Data files for the original alignment and selected sites are available from the authors on request. The maximum likelihood (ML), neighbor joining (NJ) and maximum parsimony (MP) methods for protein phylogeny were applied to the data set using the CODEML program in PAML 3.1 [36] and PROML, PROTDIST, NEIGHBOR, PROTPARS, SEQBOOT and CONSENSE programs in PHYLIP 3.6A [37]. In the ML analysis, an initial tree search was done by applying PROML with the JTT-F model for amino acid substitution process, assuming homogeneous rates across sites. Based on the best tree obtained, a Γ -shape parameter (α) of the discrete Γ -distribution with eight categories that approximates site rates was estimated by PAML. By using the α value, a further tree search with the JTT-F + Γ model with eight site rate categories was done by PROML, producing the final best tree. In the NJ analysis, ML estimates for pair wise distances among 43 sequences were calculated using PROTDIST, based on the Dayhoff PAM model with rate variation among sites allowed. The NJ tree was reconstructed from the distances using NEIGHBOR. In the MP analysis, the MP tree was searched by PROTPARS. Bootstrap analysis for each of the three methods was performed in the same way by applying PROML, PROTDIST and NEIGHBOR, or PROTPARS to 100 resampled data sets produced by SEQBOOT. Bootstrap proportion (BP) values were calculated for internal branches of the final best tree of the ML analysis by the use of CONSENSE. Trees were drawn by TREEVIEW version 1.6.0 [38].

Results

Identification of PGDH gene and its encoded protein from *E. histolytica*

We identified a putative PGDH gene (EH01468) from *E. histolytica* by homology search against the *E. histolytica* genome database using PGDH protein sequences from bacteria, plants and mammals. The putative amoebic PGDH gene contained a 900 bp ORF, which encodes a protein of 299 amino acids with a predicted molecular mass of 33.5 kDa and a pI of 8.11. No other independent contig containing the PGDH gene was found, suggesting that this PGDH gene is present as a single copy. We searched thoroughly for other possible PGDH genes using this amoebic PGDH gene in the *E. histolytica* genome database. However, no other possible PGDH-related sequence was found except for a previously described GDH gene [30].

Features of the deduced protein sequence of *E. histolytica* PGDH

The amino acid sequence of the *E. histolytica* PGDH (EhPGDH) showed 21–50% identities to PGDH from bacteria, mammals and plants. EhPGDH showed the highest amino acid identities (48–50%) to PGDH from both anaerobic intestinal bacteroides including *Bacteroides thetaiotaomicron*, *Bacteroides fragilis*, *Porphyromonas gingivalis* and a ciliate protozoan parasite living in the rumen of cattle, *Entodinium caudatum* and lowest identities (21–26%) to PGDH from higher eukaryotes including mammals and plants. For example, EhPGDH showed a 48–50% identity to PGDH from *B. thetaiotaomicron*, *E. caudatum*, *B. fragilis* and *P. gingivalis*, 35% to *Methanococcus jannaschii*, 33% to *Archaeoglobus fulgidus* and *Thermoanaerobacter tergcogensis*, 31% to *Bacillus anthracis*, *Bacillus cereus* and *Caulobacter crescentus*, 27% to *Bacillus subtilis* and *Escherichia coli*, 24–26% to human, mouse, rat, *Schizosaccharomyces pombe* and *Saccharomyces cerevisiae*, and 21% to *Arabidopsis thaliana* PGDH.

Based on the multiple sequence alignment of 35 PGDH and eight GDH sequences also used in the phylogenetic analysis (see below), PGDH sequences were classified into three types: Type I, Type II and Type III. PGDH sequences in the longest group (Type I) have a carboxyl-terminal extension of about 208–214 amino acids (Fig. 2), which is absent in those from the shortest group (Type III). The sequences with intermediate length (Type II) also possess a carboxyl-terminal extension of 73–76 amino acids, which aligned with the corresponding region of the Type I sequences. Type II sequences lack 126–135 amino acids present in Type I sequence (e.g. corresponding to residues 321–448 of *B. subtilis* PGDH). Type II sequences were further classified into Type IIA and Type IIB according to the different insertion/deletion patterns in the nucleotide binding domain. The amoebic PGDH belongs to Type III, together with those of Bacteroidales and *E. caudatum*. Type III sequences lack a region of 13–14 (in PGDH of Type I and Type IIA) or 24 amino acids (Type IIB) between Gly125 and Lys126 (of EhPGDH) in the nucleotide binding domain. The amoebic PGDH also lacks two regions present in other groups; one residue between 58 and 59 of EhPGDH (also missing in other Type III organisms and Type IIB *B. anthracis*) in the substrate binding domain and five-ten residues between amino acid 172 and 173 (Fig. 2). Type III PGDH including the amoebic PGDH lack Trp139 (amino acids numbered according to *E. coli*), which was previously shown to be implicated for cooperativity in serine binding and serine inhibition, and an adjacent Lys141/Arg141, both of which are conserved among Type I and Type II sequences. All the other important residues implicated in the active site within the substrate binding domain, as predicted from the crystal structure of *E. coli* PGDH (Arg60, Ser61, Asn108 and Gln301) [18], were conserved in EhPGDH (Arg55, Ser56, Asn102 and Asn272). A substitution of Gln272 to Asn found in EhPGDH was also shared by PGDH from *E. caudatum* and *B. thetaiotaomicron*. Arg62/Lys62, which interacts with the phosphate group of PHP [17] in Type IIA, is substituted in PGDH from the other types. The consensus sequence Gly-Xaa-Gly-Xaa₂-Gly-Xaa₁₇-Asp, involved in the binding of the adenosine

▼ Substrate binding domain

Type IIA	Escherichia coli	MAKVSLEKQIKFLLVEGVHQKALESLRAAGYTNIEFHKGALDDEQLKESIRDAHFIGL	61
	Leishmania major	MPSLIDPPYHALLLEGVNPJAKELLESKGCIVEYIPHALPROTLLEKIRDVHFLG	58
Type IIB	Bacillus anthracis	MFRTVTLNQIAEKGLQVLLGGERYEVG	39
Type I	Helicobacter pylori	MYQVAICDPIHAKGQILEAQKDIVLHDYSKCPKKE-LLEKLTPTMDALIT	51
	Synechocystis spp.	MNLAWLQGLSLGILLSPPAPALLIFRSFTMAKVLVSDSIDQVGDILTK-QVAQVDVKTGLSEAE--IIDIVEPYDAIML	77
	Bacillus subtilis	MFRVLVSDKNSNDGLQPLIESDFIEIVQKNVADAED--ELHTFDALLV	48
	Methanococcus jannaschii	MVKILYTDPLHEDIKILEEVG-EVEVATGLTKEE--LLEKIADAVLVV	49
	Archaeoglobus fulgidus	MKVLVAEPISEEAIDYMRKNGLEVEVKTGMSREE--LIREVPKYEAIVV	49
	Homo sapiens	MAFANLRKVLISDSLDPCCRKILQDGGLOVVEKQNLKSEE--LIAELQDCEGLIV	55
Type III	Bacteroides thetaiotaomicron	MKVLVATEKPFKVAVDGIRKEIEAAGYELALLEKYTKQAQ-LLDAVKDANAII	56
	Entodinium caudatum	IILLALLASINTSEILLATEKPFKTETVEDIKKLVEKSGNTFKLLEKYTKQE-LMDSIKDANAII	68
	Entamoeba histolytica	MKIVVITEKPFANAVKGIKREILEKAGHEVVMIEKYYKKED-VIERIKDAGVIV	56

▼ Nucleotide binding domain

IIA Eco	RTHLTEDVINAQKLVAGCFGIGTNOVDLAAAKRGIPVFNAPFS	TRSAVELVIGELLLLLRGVPEANAKAHRGV	IN	RLAAGSFEARQKGLG	155	
Lma	ITQVTGAILDAPLLGIGCFGIGTNOVDLYATIRGVAVFNSPFA	TRSAVELVIGEISLSRKNKTORSEEVHRGV	IN	ITHVGYEVRGKTVG	152	
IIB Ban	SLHQEELS-KDLKARAGAGVNNIPVERCTEGIVVFNTPG	ANAVKELIASLINSRRIIN	IN	GVSITKNILEGEEVPQLVESG	KQFVGSIEAGKRLG	139
I Hpy	ITPITSDFLKPLTHLKSIVRAGVGVNDIDLESCSOKGIVVMNIP	TASTIAAVELTMAHLINAVRSFPGANDQIKHQR	LK	BEDWYGTTELKNNKLG	146	
Ssp	STKVTEKIQAGSQLKIGRAGVGVNDIDVPAATRGGIVVFNAP	GSITIAAAEHALAMMARHIPPDAKNSKVESK	FE	SKQFPIGTEVYKTKTG	171	
Bsu	ATKVTEDLFNKWTSLSKIVRAGVGVNDIDIDEATKHGVIIN	APNGTITSTAEHTFAMISLNRHIIQGANISVKSRE	IE	ITAYVGSLEYGKTLG	142	
Mja	ATKVTROVIEKAELKVIIRAGVGVNDIDVEAATEKGIIVN	APDASSISVAELTMGLMLAARNIPQATASLKRGE	ED	IKRFKGIELYGKTLG	143	
Afu	ATKVDVEVINAQKLVKIVRAGVGVNDIDINAATRQGVVFN	APNGTITSTAEHTFAMISLNRHIIQGANISVKSRE	FE	SKQFPIGTEVYKTKTG	142	
Hsa	ATKVTADVINAQKLVKIVRAGVGVNDIDVLEAATRKGIV	VNTPNGTISAAELTCGMINCLAROIPQATASMKDGG	KE	IKKFMGTELNGKTLG	149	
III Bth	SIIDAELVDAAKELKIVRAGAGYDNVDLAAATAHNVVCMNT	PGTISNAVAELALGMNVYAVRNFYNGT	IN	SGTELKGGKGLG	136	
Eca	SK-ITKEIMDSSNMLKVIARAGAGFNDIDLGAYASKGIV	VNNTPGTISNAVAELVFGLLVYAKRNFYDGS	IN	SGTELKGGKGLG	148	
Ehi	SK-IDEEIKAGEKVKIIVRAGAGYDNIDIEACNOGKIVMN	TPGTRNGVAELCGIMNIFGRKGFKEG	IN	KGRELDKDTLG	136	

IIB Ban	VIGLRAIGALVANDALALGMDVGVGPPYISVETAWRLSTH	VORAFSLDEIFATQDYLHPLNTOIKGIMGEHAVEKMKKGMRL	FNFSRGLVDEKVLQKALEEIIAH	249	
I Hpy	IIGFNIIGSRVGIKAKAFEMVLAYPPYIPSSKATQGLVIT	YTKN-FEDILQ-CDMJIHTPKNKEIINMIKAKEIEMKKGVI	LLNCAAGGLYNEDALYEALETKKVWR	253	
Ssp	VVGLKIGSHVAGVAKAMGMKLLAYPPISQERADQIGTCL	VD-LDLLFSEADFITLHPKPTETANLINAETLAKMKPTAR	IINCSGGIIDEEALVTALETAQIGG	278	
Bsu	IVGLERTISEIAQRGAFGMTVHVFDPFLTEERAKKIGVS	RTEFEEVLESADITVHTPLTKETKGLLNKETIAKTKKGVRL	INCAGGIIIDEAALLEALENHGVAG	249	
Mja	VIGLIRIGDQGVKRAKAFGMNIIIGYDPIYKVEAESMG	VELVOD-INELCKRADFITLVHPLTPKTRHIIGREDIAL	MKNNAIIVNCAAGGLIDEKALYEALKEGIR	251	
Afu	VIGLIRVFEFAKRCCKALGMVLAAYPPVSKERAEGV	KLVVD-FDTLLASDDVITVHVPRTKETIGLIGKGF	EKNKDGVIIVNNAAGGIIDEAALLEALYKAGVAA	250	
Hsa	ILGLRIGREAVATRMQSGFMKTIIGYDPIISPEVAS	AFGVQQLP-LEEIWPICDFITVHTPLLPSTGLLNDNT	FAQQCKGVRVWNCAGGIVDEGALLRALKQSGDCA	256	
III Bth	ILGRIYRNRVARVAKGFMVEVYAYDFQPKVEIEKDG	VKALDS-AEELYKIQVVSLHIIPATAETKNSINYALL	KDMPKGMMLVNTARKEVINAEELIKLMEDRADFK	244	
Eca	LLAFNVYRNRVARAKGFMGIYSYDAFVPKVELEKEGI	HAVDK-OEDLFTDQDIVSLHIIPATKETINSINYDL	CSKMKKNAIILINTSKVEIINKELIKLMERKDIK	256	
Ehi	IGCCYVGRKVKIEAGISMKIKVYDFFITTENQVK	-----IEELFEECOVLSLHLPLTKETKGI	GYELIKKLPYGMICNTAKKEIIDEEGLIRIMRERED	1	237

▼ Substrate binding domain

IIB Ban	YVTD-FPNH-----VIKKNVATATP	ILGASTSESENCACVMAARQLREYLETGNIRNSVNYPN	VELPYIG	314	
I Hpy	LGIQVFSKCPGIIH-----NKLLDLPVYATP	IIICANTLESHEEISKQAAGGVMSLGGSSPHALNLP	QAFD-ASAKAYLNLQAKLGYFSSQIHKGVCQKIELSLCG	355	
Ssp	AALVFAGEPLG-----ESRLREFSNVILTP	ILGASTEEAVNVAVDVAEIDRDLGLPARSAVINPGL	TPDVMKELRPYLKLAETIGTLVGLLAGGRIDRLTVCLQG	382	
Bsu	AALVFVEPPPV-----DNKLVDHPLVITATP	ILGASTKEALNVAAQVSEELQFAGKLPVMSAINLP	PAMTKDEFKIKPYHOIAGKIGSLVSOQMKEPVQDAVIQ	353	
Mja	AALVFEEPPPK-----DNPLLTLDNVI	GTPILGASTTEEAQKAAGTIVAEQIKKVLRGELAE	VNVNMPNIPQEKGLKPYMLLAELMGNINMVLQDGS	VNRELIVSG	355
Afu	AALVYKPPPS-----PDNPLKLDNVVITP	IIIGASTREALNVGMIIAEDIVNMAKGLPVRNAV	NLPSIEPSDFEENMPLFLAEKMGKIASVRLGGA	IRKVKVTCSSG	355
Hsa	AALVFTEPPR-----DRALVDHENVISCP	ILGASTKEASRSGEEIAVQFVDMVKGKSLTG	VVNAQALTSAFSPHTKPIIQLAELGTLMRAHAG	SPKGTIOVITQG	360
III Bth	YMTDIMPANAEEF-----AEKFAQ-RYFSTPK	CAQTAEASINAGIAAAQIVGLKDGCEKFRV	NK-306		
Eca	YITDLKPDVHEEF-----LNKFKG-RYFATPK	CAQTQEAIIINAGKAAANOIIDFFKTG	KTKFVNK-318		
Ehi	YITDVAQ-ISKVF-----NNEFKG-RFFATP	IIIGAEATEESINAGMAASQIICDFFTNG	VKVFVNK-299		

IIB Ban	YVTD-FPNH-----VIKKNVATATP	ILGASTSESENCACVMAARQLREYLETGNIRNSVNYPN	VELPYIG	314	
I Hpy	LGIQVFSKCPGIIH-----NKLLDLPVYATP	IIICANTLESHEEISKQAAGGVMSLGGSSPHALNLP	QAFD-ASAKAYLNLQAKLGYFSSQIHKGVCQKIELSLCG	355	
Ssp	AALVFAGEPLG-----ESRLREFSNVILTP	ILGASTEEAVNVAVDVAEIDRDLGLPARSAVINPGL	TPDVMKELRPYLKLAETIGTLVGLLAGGRIDRLTVCLQG	382	
Bsu	AALVFVEPPPV-----DNKLVDHPLVITATP	ILGASTKEALNVAAQVSEELQFAGKLPVMSAINLP	PAMTKDEFKIKPYHOIAGKIGSLVSOQMKEPVQDAVIQ	353	
Mja	AALVFEEPPPK-----DNPLLTLDNVI	GTPILGASTTEEAQKAAGTIVAEQIKKVLRGELAE	VNVNMPNIPQEKGLKPYMLLAELMGNINMVLQDGS	VNRELIVSG	355
Afu	AALVYKPPPS-----PDNPLKLDNVVITP	IIIGASTREALNVGMIIAEDIVNMAKGLPVRNAV	NLPSIEPSDFEENMPLFLAEKMGKIASVRLGGA	IRKVKVTCSSG	355
Hsa	AALVFTEPPR-----DRALVDHENVISCP	ILGASTKEASRSGEEIAVQFVDMVKGKSLTG	VVNAQALTSAFSPHTKPIIQLAELGTLMRAHAG	SPKGTIOVITQG	360

Regulatory domain

IIB Ban	IMHQNVPNMVGQITGLCAEHHINIDM	INRS--KHSWAYTIMIDNIGIDDIKENI	VENISKITGVAVRMIV	390				
I Hpy	FRNTDIPGVI	GSVGNFAFRHGINIDFRLGR--	NTQKEALALIIIVDEEVSELEVLEELKN	IPACL	SVHYVVI--	524		
Ssp	TLHRDMPGI	IGKIGSLGSGFNVI	ASMQVGR--KIVR	GDAIMALSLDPLPDGLLSEITK	VAGIRDAYTVKL--	554		
Bsu	IOHDDTGT	IGRVGIRLGDNDINI	ATMQVGR--KEKGG	EIMMLSFDRHLEDKIVKELT	NVPDIVSVK	IDLP--	525	
Mja	IKHIDRPGT	IGRVCITLGDYGINI	ASMQVGR--KEPG	GSVMLNLNDHTVPEVIEK	IKENIPN	IKDVA	INL--	524
Afu	SLHEDKPGV	IGVGTGLFRNNINI	AGMIVGR	SGDKPGGIGLMLL	VDDPPTPEVLEEMTKL	GDIDATY	VEL--	527
Hsa	RTGTSDPAMLPTM	IGLAEAGVRLLSYOTS	L--VSD	GETWHVMISSL	LPSLEAWKHQVTEAF	QHFH-----	533	

portion of NAD⁺ [39], is located between amino acids 139–162 of EhPGDH. The His292 and Glu269, conserved among Type I and Type II PGDH, were substituted with lysine and threonine, respectively, in EhPGDH; identical or similar substitutions were also observed in Type III PGDH from *E. caudatum* and *B. thetaiotaomicron*. In contrast, Arg240 and Asp264, also implicated for substrate binding [40,41], are totally conserved in all organisms. Gly294, located at the junction of the substrate and nucleotide binding domains, forms the active site cleft and is involved in substrate binding and serine inhibition as shown previously with the Gly294Ala or Val mutation, which affected K_m and cooperativity of serine inhibition [42].

We also searched for putative PGDH encoding genes in the genome and expressed sequence tag databases of other parasitic protozoa including *Leishmania*, *Plasmodium*, *Giardia*, *Trypanosoma*, *Toxoplasma*, *Schistosoma*, *Theileria*, *Cryptosporidium*, *Eimeria*, *Trichomonas* and nonparasitic protozoan *Dictyostellium discoideum*, but did not find orthologues in these databases except for *Leishmania*, suggesting that PGDH may be exclusively present in only a limited group of protozoa. However, as most of these genomes have not been fully sequenced, a unique presence of PGDH in *E. histolytica*, *Leishmania* and *E. caudatum* among protozoa cannot be ensured.

Phylogenetic analysis

The phylogenetic inference was performed by ML, NJ and MP methods using protein sequences from 35 PGDH and eight GDH from various organisms. We also reconstructed phylogenetic trees using only 35 PGDH sequences after removing GDH sequences. The results were very similar to those created with both PGDH and GDH sequences (data not shown). The three methods consistently reconstructed the monophyly of Type IIA, Type IIB and Type III with 100% BP supports as shown in the ML tree with the JTT-F + Γ model (Fig. 3). The monophyly of GDH, a close relationship of Type IIA with GDH, and a sister group relationship between Type IIB and Type III were also reconstructed consistently among different methods,

although no clear BP supports were obtained except for the latter relationship in the NJ analysis (88%, Fig. 3). The ML tree demonstrates that the common ancestor of Type IIB and Type III is located within Type I and it branches off from the line leading to ϵ -proteobacteria. Various prokaryotic groups including α -, δ - and ϵ -proteobacteria, cyanobacteria, Clostridiales, Actinomycetales and archaeobacteria belong to Type I, while β - and γ -proteobacteria and Bacteroidales belong to Type IIA and Type III, respectively. It is worth noting that Bacillales are not monophyletic in the tree. A clade consisting of *B. subtilis* and *B. halodulans* and an independent branch for *S. epidermidis* are located separately in Type I, whereas *B. cereus* and *B. anthracis* belong to an independent clade, which was regarded as Type IIB according to the alignment mentioned above. No monophyletic origin was observed for eukaryotic PGDH sequences. Mammals and plants are independently located in Type I. Fungi form a monophyletic clade together with *Leishmania* in Type IIA. *E. histolytica* PGDH is located at the basal position of Type III, which is followed by stepwise emergence of a ciliate protozoan, *E. caudatum*, and three Bacteroidales. No part of the PGDH/GDH tree is comparable with an accepted organismal phylogeny as inferred mainly from small subunit rRNA sequences, demonstrating that many lateral gene transfer events, together with drastic insertion/deletion events, occurred during the evolution of PGDH/GDH, and made their evolutionary history complicated. A close phylogenetic association between EhPGDH and PGDH from Bacteroidales suggests that the amoebic PGDH was obtained from an ancestral organism of bacteroides by lateral gene transfer as suggested for fermentation enzymes (from archaea and bacteria) [43,44] and for GDH (from ϵ -proteobacteria) [30], or, in contrast, that Bacteroidales obtained the gene from *E. histolytica* or *E. caudatum*.

Purification and characterization of rEhPGDH

The recombinant EhPGDH (rEhPGDH) protein revealed an apparently homogeneous band of 35 kDa on an SDS/PAGE gel electrophoresed under the reducing condition (Fig. 4), which was consistent with the predicted size of the deduced monomer of EhPGDH protein with the extra 20 amino acids added at the amino terminus. The purified rEhPGDH protein was evaluated to be > 95% pure as determined on a Coomassie-stained SDS/PAGE gel. We first optimized conditions for enzymatic assays, i.e. pH, salt concentrations, requirement of cofactors, divalent metal ions, dithiothreitol and stabilizing reagents. rEhPGDH was unstable and the enzyme was totally inactivated when stored without any preservative or additive at room temperature, 4 or -20 °C overnight, which was similar to pea PGDH. The pea PGDH activity was stabilized in the presence of 2.5 M glycerol or 100 mM 2-mercaptoethanol [9]. Similarly, when rEhPGDH was stored in 50 mM Tris/HCl buffer, pH 8.0 containing 50% (v/v) glycerol at -80 °C, rEhPGDH remained fully active for more than one month. The maximum activity of rEhPGDH for the forward reaction (forming PHP) was observed at slightly basic pH (pH 9.0–9.5), which decreased substantially with lower pH (results not shown). The PGDH activity in the reverse reaction (forming 3-PGA) was greatly affected by variations of pH; the activity was found highest at slightly acidic pH (pH 6.0–6.5).

Fig. 2. Multiple alignments of deduced amino acid sequences of PGDH from various organisms including *Entamoeba histolytica*. Based on the multiple sequence alignment of 35 PGDH and eight GDH sequences, PGDH sequences were classified into four types: Type I, Type IIA, Type IIB and Type III (see text). Only 12 sequences from representative organisms that belong to each type are selected and shown in this alignment. Fig. 3 details accession numbers. Asterisks indicate identical amino acids. Dots and colons indicate strong and weaker conservations, respectively (<http://clustalw.genome.jp/SIT/clustalw.html>). Dashes indicate gaps. Functional domains implicated for catalysis of *E. coli* PGDH are shown over the alignment, where junctions between the domains are depicted by ▼. An open box in the nucleotide binding domain indicates the NAD⁺-binding domain (Gly-Xaa-Gly-Xaa₂-Gly-Xaa₁₇-Asp) and all conserved residues implicated for the NAD⁺ binding are inverted (white text on black shading). Grey shading indicates the conserved amino acids that participate in the substrate and nucleotide binding during catalysis of *E. coli* PGDH. Open boxes with dotted lines indicate significant gap regions with > 10-residue insertions/deletions.

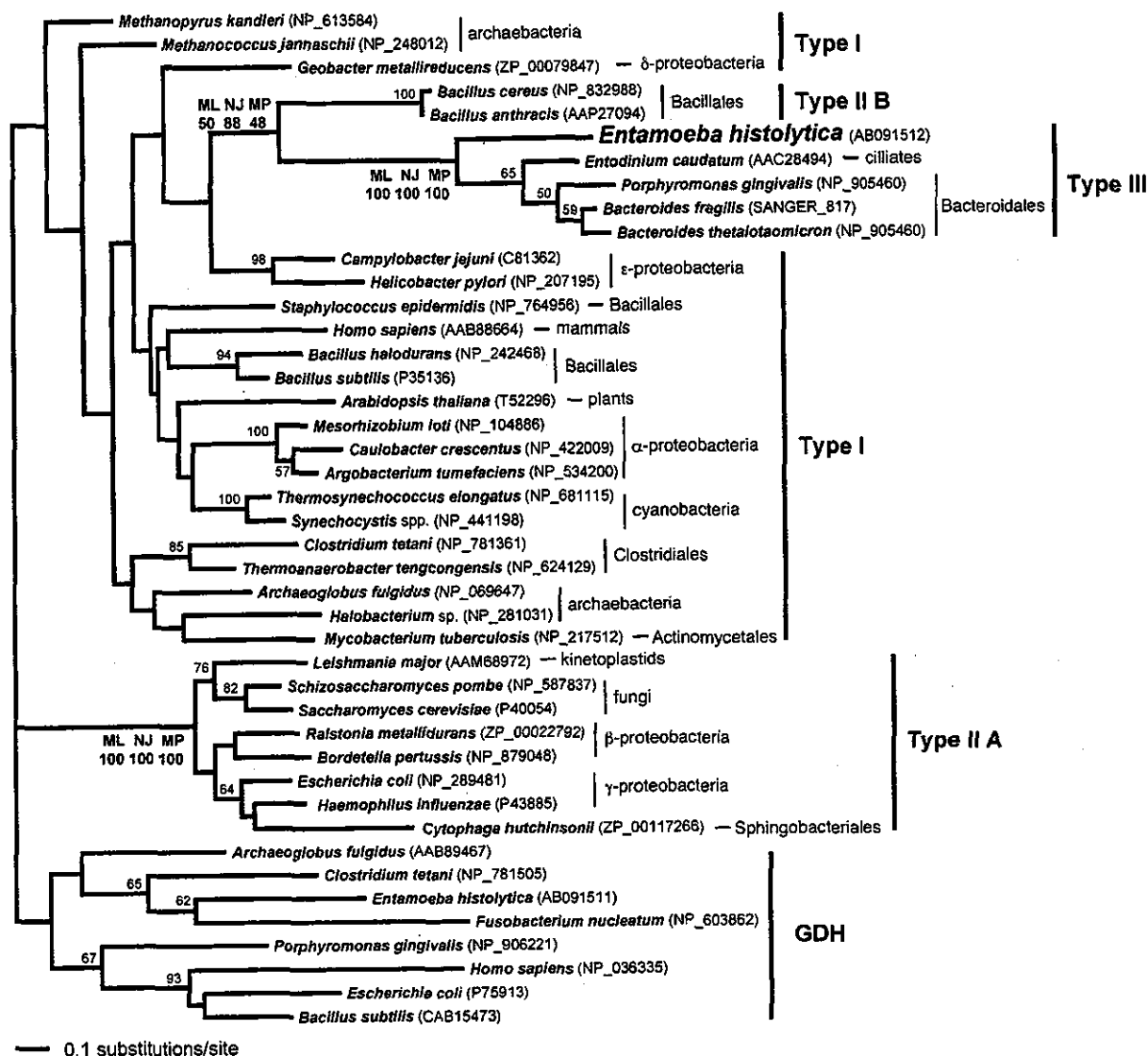


Fig. 3. Composite phylogenetic tree of PGDH and GDH sequences. The best tree finally selected by the ML analysis with the JTT-F + Γ model is shown. The α value of the Γ -shape parameter used in the analysis is 1.283. Bootstrap proportions (BPs) by the ML method are attached to the internal branches. Unmarked branches have < 50% BP. For the three nodes of interest, BP values by the NJ and MP methods are also shown. The length of each branch is proportional to the estimated number of substitutions. One hundred and eighty two amino acid positions that were unambiguously aligned among 35 PGDH and eight GDH sequences were selected and used for phylogenetic analysis. These correspond to the residues 70–121, 130–159, 174–244, 257–261 and 263–287 of the *E. histolytica* PGDH sequences. The *Bacteroides fragilis* PGDH sequence was deduced from the nucleotide positions between 2426073 and 2426993 of SANGER_817.

Dissimilarly to PGDH from bacteria [8] and plant [13], substrate inhibition of EhPGDH by PHP was observed at > 10 μM and reversed by the addition of salt (100–400 mM NaCl) at various NADPH/NADH concentrations (40–200 μM), as reported for rat liver PGDH [13]. The optimum salt concentration for rEhPGDH was determined to be 350–400 mM NaCl or KCl. Neither dithiothreitol nor EDTA showed any significant effect on the EhPGDH activity.

Kinetic properties of rEhPGDH

Owing to the apparent stimulatory effect of salt on rEhPGDH activity, as described above, we conducted

further kinetic studies in the presence of 400 mM NaCl. At saturating concentrations of the substrate, rEhPGDH showed an approximately eightfold higher affinity to NADH than NADPH, and specific activity was about threefold higher with NADH than with NADPH in the reverse direction (Table 1). The K_m for 3-PGA and NAD⁺ in the forward reaction was calculated to be one order higher than those for PHP and NADH in the reverse reaction. We did not observe utilization of NADP⁺ in the forward reaction even in the presence of high concentrations of NADP⁺ (0.4 mM) and 3-PGA (5–10 mM). K_m for substrates of EhPGDH was similar to that of mammalian PGDH [11,13], and one to two orders lower than that of

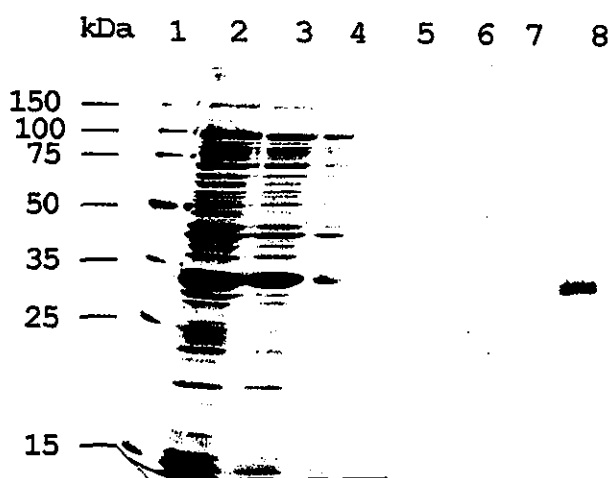


Fig. 4. Expression and purification of recombinant EhPGDH protein. EhPGDH protein was expressed as fusion protein using pET-15b expression vector and purified with Ni^{2+} -nitrilotriacetic acid column as described in Materials and methods. A total cell lysate and samples in each purification step were electrophoresed on 12% SDS/PAGE gel and stained with Coomassie Brilliant Blue. Lane 1, protein marker; lane 2, a total cell lysate; lane 3, a supernatant of the total lysate after 24 000 g centrifugation; lane 4, an unbound fraction; lanes 5–8, fractions eluted with 20, 35, 50 and 100 mM imidazole, respectively.

Table 1. Kinetic parameters of recombinant EhPGDH. The kinetic parameters of EhPGDH were determined as described in Materials and methods. Mean \pm SD of two-to-four independent measurements are shown. ND, not determined.

Substrate/cofactor	pH	K_m (μM)	Specific activity ($\mu\text{mol}\cdot\text{min}^{-1}\cdot\text{mg protein}^{-1}$)
Phosphohydroxypyruvate ^a	6.5	15.0 ± 1.02	16.7 ± 1.07
NADH ^b	6.5	17.7 ± 2.52	7.69 ± 0.76
NADPH ^b	6.5	141 ± 9.02	2.71 ± 0.27
3-Phosphoglycerate ^c	9.0	212 ± 12.6	0.83 ± 0.02
NAD ⁺ ^d	9.0	86.7 ± 5.77	1.34 ± 0.08
NADP ⁺ ^e	9.0	ND	ND

^a 0.2 mM NADH used, ^b 0.1 mM PHP used, ^c 0.2 mM NAD⁺ used, ^d 3.0 mM 3-phosphoglycerate used, ^e 0.4 mM NADP⁺ and 5–10 mM 3-phosphoglycerate used.

bacterial PGDH [7]. Although PGDH from *E. coli* was shown to utilize 2-oxoglutarate as substrate to produce hydroxyglutarate [45], the amoebic PGDH did not utilize this substrate up to 5 mM either in the presence or absence of 400 mM NaCl (results not shown). Thus, the amoebic PGDH appeared to be specific for the PHP-3-PGA conversion, similar to the rat liver PGDH [13]. We also tested whether serine, which was shown to inhibit the activity of PGDH from *E. coli* [7], *B. subtilis* [8] and a plant [9], affects PGDH activity in both the forward and reverse directions. In addition, we tested other amino acids, i.e. Ala, Cys, Gly, Val, Met, Trp, Thr, *O*-acetylserine, *N*-acetylserine, DL-homoserine and DL-homocysteine. However, none of these amino acids, at 10 mM, affected the enzymatic activity of EhPGDH. No effect was observed by preincubation of

the enzyme with serine (1–10 mM) in the presence of dithiothreitol. The native EhPGDH was also not affected by up to 10 mM L-serine.

Chromatographic separation of the native and recombinant EhPGDH activities

In order to correlate native PGDH activity in the *E. histolytica* lysate with the recombinant enzyme, the lysate from the trophozoites and rEhPGDH were subjected to chromatographic separation on a Mono Q anion exchange column (Fig. 5). The *E. histolytica* total lysate showed PGDH activity of 26.6 nmol NADH utilized per min per mg lysate protein in the reverse direction. Thus, native PGDH

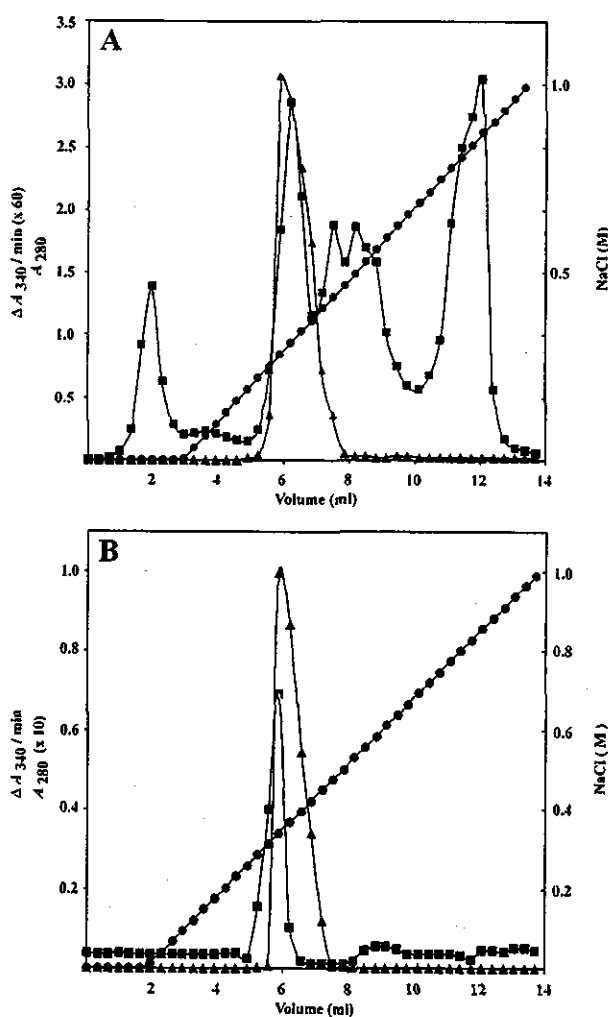


Fig. 5. Separation of the native EhPGDH from the *E. histolytica* trophozoites and rEhPGDH by Mono Q anion exchange chromatography. (A) Elution profile of the native EhPGDH. The total lysate of *E. histolytica* trophozoites was separated on the anion exchange column at pH 9.0 with a linear gradient of NaCl (0–1.0 M). (B) Elution profile of the recombinant PGDH protein. The rEhPGDH protein was dialyzed against the binding buffer and fractionated under the identical condition. ■, the absorbance at 280 nm; ▲, EhPGDH activity shown by a decrease in the absorbance at 340 nm (min^{-1} (60-fold)); ●, NaCl concentration of a linear gradient.

represents 0.2–0.4% of a total soluble protein, assuming that native and recombinant EhPGDH possess a comparable specific activity. *E. coli* was shown to possess a comparable amount of PGDH, which constitutes about 0.25% of the total soluble protein [7]. The PGDH activity was eluted as a single peak at an identical salt concentration for both native and recombinant EhPGDH. This finding, together with the fact that the *PGDH* gene is present as a single copy, indicates that the *EhPGDH* gene we cloned represents the dominant and, probably, sole gene responsible for PGDH activity in this parasite. To obtain an insight on the multimeric structure, the recombinant PGDH enzyme was subjected to gel filtration chromatography. The PGDH activity was eluted at the predicted molecular size of 70–74 kDa (data not shown). This is consistent with a notion that rEhPGDH exists as a dimer with a monomer consisting of 33.5 kDa plus 2.6 kDa. This observation suggests that the amoebic PGDH enzyme exists as a homodimer, which is different from PGDH from all other organisms previously reported.

Discussion

In the present study, we have demonstrated that the enteric protozoan parasite *E. histolytica* possesses one of the key enzymes of the phosphorylated serine metabolic pathway. As far as we are concerned, this is the first demonstration of PGDH and the presence of the phosphorylated serine pathway in unicellular eukaryotes including parasitic and nonparasitic protists. Taken together with our previous demonstration of GDH, which is involved in the nonphosphorylated pathway for serine degradation [30], this anaerobic parasite probably possesses dual pathways for serine metabolism. PGDH has been shown to play an essential role in serine biosynthesis in human, but not in degradation, as demonstrated in the genetic diseases caused by its deficiency [12,21–23]. We propose, based on the following biochemical evidence, that this enzyme also plays a key role in serine biosynthesis in *E. histolytica*.

The kinetic parameters of EhPGDH did not necessarily support that the forward (in the direction of serine synthesis) reaction is favoured over the reverse reaction. The amoebic PGDH showed a strong preference toward NADH compared to NAD^+ (\approx fivefold higher K_m for NAD^+ than NADH) (Table 1). Furthermore, the amoebic PGDH showed an \approx 14-fold higher affinity and \approx 20-fold higher specific activity to PHP than 3-PGA, which are similar to animal, plant and bacterial enzymes [3,7,8,13]. However, a few lines of evidence support the hypothesis that under physiological conditions, the forward reaction is favoured. First, intracellular concentration of NAD^+ is generally much higher than that of NADH in the cell: e.g. the free NAD^+ /free NADH ratio in the rat liver cytoplasm was shown to be 725 : 1 [46]. Secondly, 3-PGA, an essential intermediate of the glycolytic pathway, is present at a high concentration [$0.3 \mu\text{mol} \cdot (\text{g wet weight rat liver})^{-1}$] [47] compared to the concentration of PHP [$0.085 \text{ nmol} \cdot (\text{g wet weight rat brain})^{-1}$] [48]. Finally, the last step of the phosphorylated pathway (conversion of 3-*O*-phosphoserine to serine catalyzed by a putative phosphoserine phosphatase) is unidirectional.

As far as the present data are concerned, a gene encoding PGDH appears to be absent in other parasitic and nonparasitic protists, including *Plasmodium*, *Giardia*, *Trypanosoma*, *Trichomonas*, *Toxoplasma*, *Schistosoma*, *Cryptosporidium* and *D. discoideum*, although genome sequence databases of some of these organisms are still incomplete. Because the genome database from *E. caudatum* is not currently available, we cannot rule out a possibility that this ciliate protozoan also possesses the nonphosphorylated pathway. The presence of the phosphorylated serine metabolic pathway may be limited only to *E. histolytica* and *Leishmania*, a representative member of a group of unicellular hemoflagellates which resides in the cytoplasmic vacuoles of mammalian macrophages and in the digestive tract of insects, and *E. caudatum*, an anaerobic protozoan ciliate living in the cattle rumen. However, *Leishmania* and *Entamoeba/Entodinium* PGDH belong to divergent PGDH groups (Type IIB and Type III, respectively), and thus their origins appear to be distinct, as also inferred by phylogenetic reconstructions (Fig. 3). This differential presence and inheritance is satisfactorily explained by a differential loss/retention model, i.e. some protists including *E. histolytica*, *E. caudatum* and bacteroides acquired Type III PGDH while *Leishmania*, fungi, β - and γ -proteobacteria inherited Type IIA PGDH. Sequence alignment indicated that PGDH from Bacteroidales, *E. caudatum* and *E. histolytica* are grouped together as Type III sequences, which lack both the conserved Trp139 in the nucleotide binding domain and the carboxyl-terminal extension implicated for allosteric feedback inhibition of the *E. coli* PGDH (Fig. 2). Phylogenetic analysis also demonstrated clearly the monophyletic origin of these sequences with 100% BP support (Fig. 3). It is therefore reasonable to propose that the human intestinal parasite *E. histolytica*, and *E. caudatum*, an anaerobic protist living in rumen of cattle, sheep, goats and other ruminants, gained the Type III PGDH gene from the Gram-negative anaerobic bacteroides or their ancestral organisms which also reside in the mammalian guts. However, an alternative possibility could not be ruled out that lateral gene transfer event(s) occurred in the opposite direction from *E. histolytica* or *E. caudatum* to Bacteroidales. It should be examined in the future whether *E. caudatum* and *B. thetaiotaomicron* PGDH possess biochemical properties similar to the amoebic PGDH. This poses a possibility that PGDH and the phosphorylated serine pathway may be involved in cellular metabolism associated with anaerobic metabolism as previously discussed for GDH [30]. Disclosure of the entire genome data of other anaerobic protists, e.g. *Trichomonas* and *Giardia*, should address this question. We must also mention that one should be cautious with such inferences of pervasive lateral gene transfer and differential gene loss/retention as possible causes of an observed aberrant overall tree topology as shown by our phylogenetic analyses. The observed phylogenetic relationship is also explained by unrecognized paralogies and homoplasy (e.g. a convergence to common function). It is also worth noting the small length of alignment that was used in our analyses (180 positions) and there is also a possibility of mutational saturation.

Parasitic protists are generally known to possess a simplified amino acid metabolism. For instance, the human

malaria parasite *Plasmodium falciparum*, which resides in erythrocytes in mammals, possess only a limited set of enzymes involved in amino acid synthesis of Ser from Gly and Ala from Cys and conversions between Asp and Asn and between Glu and Gln [49]. Serine metabolic pathways are often absent in parasitic protists; the majority of these protists, as mentioned above, apparently lack both of the serine pathways based on their genome data. There are two exceptions: *E. histolytica* possesses both serine metabolic pathways, and *Leishmania* has the phosphorylated pathway, but not the nonphosphorylated pathway. It is not understood why *E. histolytica* retains both of the serine metabolic pathways. However, it is conceivable to speculate that serine metabolism plays such a critical role that dual pathways are retained in this parasite. Serine is involved both (a) in the production of pyruvate by serine dehydratase, associated with energy metabolism [50], and (b) in biosynthesis of cysteine, which is essential for growth, survival, attachment [28,29] and antioxidative defense [27] of this parasite. The presence of the nonphosphorylated serine pathway, which we previously proposed to play a role in serine degradation, also reinforces our premise on the physiological essentiality of serine metabolism in this parasite. It was previously shown that all three enzymes of the phosphorylated pathway were induced by protein-poor, carbohydrate-rich diet in the liver [14,51]; e.g. 12-fold increase of PGDH and 20-fold increase of PSAT activity were observed in rat liver [47]. In contrast, the intraperitoneal administration of cysteine (0.5 mM) caused a 50% decrease and complete loss of PGDH mRNA expression in rat liver within eight and 24 h, respectively [14]. These data indicate, by analogy, that serine biosynthesis may also be regulated to maintain the intracellular cysteine concentration in the amoeba. Modulation of expression of PGDH and other enzymes involved in the phosphorylated pathway by cultivation of the amoebic trophozoites with a variety of amino acids is underway.

It was previously shown that dimerization and tetramerization of *E. coli* PGDH involves interaction between the nucleotide binding domain and between the regulatory domains, located at the central and carboxyl terminus, respectively, of the two adjacent subunits [18,52]. The conserved Trp139 of the nucleotide binding domain from *E. coli* was shown to play an important role in the tetramerization and also in the cooperativity and inhibition by serine [17,52]. Its side chain was shown to be inserted into the hydrophobic pocket of the nucleotide binding domain of one of the adjacent subunits. Site directed mutagenesis of Trp139 to Gly resulted in the dissociation of the tetramer to a pair of dimers and in the loss of cooperativity in serine binding and inhibition [17,52]. The truncated variant of rat liver PGDH, which lacks the carboxyl-terminal domain, was shown to form a homodimer but not a tetramer [13]. In contrast to this report, a recent report has shown that the removal of the regulatory domain was sufficient to eliminate serine inhibition, but did not affect tetramerization [53]. The EhPGDH lacks both the conserved Trp139 and the carboxyl-terminal regulatory domain. These facts, based on the primary structure, appear to be sufficient to explain a homodimeric structure of the amoebic PGDH as shown by gel filtration. It is probable that not only Trp139 but

also adjacent amino acids of this region presumably forming α -helix contribute to tetramerization of PGDH from other organisms. The active site of PGDH contains conserved positively charged amino acids, i.e. Arg60, Arg240 and Arg141/Lys141, whose side chains protrude into the solvent accessible space of the active site cleft and are thought to be responsible for the binding to 3-PGA, which is highly negatively charged with the phosphate and carboxyl groups [17]. The amoebic PGDH also contains Arg55 and Arg217, but lacks Arg141/Lys141, which might partially explain a reduced affinity of the amoebic PGDH for PHP (K_m of *E. coli* PGDH for PHP was one order lower than that of the amoebic PGDH). In addition, Arg62/Lys62 is substituted with Asp in Type III PGDH, which may also contribute to the observed reduced affinity to PHP, as previously shown in the mutational study (Arg62Ala) for *E. coli* PGDH [17]. The Asp-His pair or Glu-His pair, which makes up the so-called charge relay system, was previously implicated for efficient catalysis for many dehydrogenases [40,41]. The important residues implicated in the pairing in the active site histidine/carboxylate couple, as predicted from the crystal structure of *E. coli* PGDH (Arg240, Asp264, Glu269 and His292) [18] were almost identical in EhPGDH (Arg217, Asp241 and Lys263), but Glu269 was substituted with an uncharged amino acid Thr245 (in *E. histolytica*), similarly to *B. thetaiotaomicron* PGDH (Ala253) and *E. caudatum* PGDH (Asn265), respectively. His292 of *E. coli* PGDH was replaced with positively charged Lys263 in PGDH from *E. histolytica*, *E. caudatum* and *B. thetaiotaomicron*. It is worth noting that His187 in EhPGDH (His210 of *E. coli*) is totally conserved in all 35 organisms (results not shown), suggesting the importance of this residue. We are currently examining a role of His187 in the proton relay system by mutational studies.

Acknowledgements

We thank Shin-ichiro Kawazu and Shigeyuki Kano, International Medical Center of Japan, for providing the Fluorometer and helpful discussions. This work was supported by a grant for Precursory Research for Embryonic Science and Technology, Japan Science and Technology Agency to T. N., a fellowship from the Japan Society for the Promotion of Science to V. A. (No. PB01155), a grant for research on emerging and re-emerging infectious diseases from the Ministry of Health, Labour and Welfare of Japan to T. N., Grant-in-Aid for Scientific Research on Priority Areas from the Ministry of Education, Culture, Sports, Science and Technology of Japan to T. N. (15019120, 15590378), and a grant for Research on Health Sciences Focusing on Drug Innovation from the Japan Health Sciences Foundation to T. N. (SA14706).

References

1. Snell, K. (1984) Enzymes of serine metabolism in normal, developing and neoplastic rat tissues. *Adv. Enzyme Regul.* **22**, 325–400.
2. Snyder, S.H. & Kim, P.M. (2000) D-amino acids as putative neurotransmitters: focus on D-serine. *Neurochem. Res.* **25**, 553–560.
3. Ho, C.L., Noji, M., Saito, M. & Saito, K. (1999) Regulation of serine biosynthesis in *Arabidopsis*. Crucial role of plastidic 3-phosphoglycerate dehydrogenase in non-photosynthetic tissues. *J. Biol. Chem.* **274**, 397–402.

4. Srinivasan, R. & Oliver, D.J. (1995) Light-dependent and tissue-specific expression of the H-protein of the glycine decarboxylase complex. *Plant Physiol.* **109**, 161–168.
5. Ho, C.L. & Saito, K. (2001) Molecular biology of the plastidic phosphorylated serine biosynthetic pathway in *Arabidopsis thaliana*. *Amino Acids* **20**, 243–259.
6. Snell, K. (1986) The duality of pathways for serine biosynthesis is a fallacy. *Trends Biochem. Sci.* **11**, 241–243.
7. Sugimoto, E. & Pizer, L.I. (1968) The mechanism of end product inhibition of serine biosynthesis. I. Purification and kinetics of phosphoglycerate dehydrogenase. *J. Biol. Chem.* **243**, 2081–2089.
8. Sasaki, R. & Pizer, L.I. (1975) Regulatory properties of purified 3-phosphoglycerate dehydrogenase from *Bacillus subtilis*. *Eur. J. Biochem.* **51**, 415–427.
9. Slaughter, J.C. & Davies, D.D. (1968) Inhibition of 3-phosphoglycerate dehydrogenase by L-serine. *Biochem. J.* **109**, 749–755.
10. Larsson, C. & Albertsson, E. (1979) Enzymes related to serine synthesis in spinach chloroplasts. *Physiol. Plant.* **45**, 7–10.
11. Walsh, D.A. & Sallach, H.J. (1965) Purification and properties of chicken liver D-3-phosphoglycerate dehydrogenase. *Biochemistry* **4**, 1076–1085.
12. Jaeken, J., Dethoux, M., Van Maldergem, L., Frijns, J.P., Alliet, P., Foulon, M., Carchon, H. & Van Schaftingen, E. (1996) 3-Phosphoglycerate dehydrogenase deficiency and 3-phosphoserine phosphatase deficiency: inborn errors of serine biosynthesis. *J. Inher. Metab. Dis.* **19**, 223–226.
13. Achouri, Y., Rider, M.H., Schaftingen, E.V. & Robbi, M. (1997) Cloning, sequencing and expression of rat liver 3-phosphoglycerate dehydrogenase. *Biochem. J.* **323**, 365–370.
14. Achouri, Y., Robbi, M. & Van Schaftingen, E. (1999) Role of cysteine in the dietary control of the expression of 3-phosphoglycerate dehydrogenase in rat liver. *Biochem. J.* **344**, 15–21.
15. Winicov, I. & Pizer, L.I. (1974) The mechanism of end product inhibition of serine biosynthesis. IV. Subunit structure of phosphoglycerate dehydrogenase and steady state kinetic studies of phosphoglycerate oxidation. *J. Biol. Chem.* **249**, 1348–1355.
16. Schuller, D.J., Fetter, C.H., Banaszak, L.J. & Grant, G.A. (1989) Enhanced expression of the *Escherichia coli* serA gene in a plasmid vector. Purification, crystallization, and preliminary X-ray data of D-3 phosphoglycerate dehydrogenase. *J. Biol. Chem.* **264**, 2645–2648.
17. Grant, G.A., Kim, S.J., Xu, X.L. & Hu, Z. (1999) The contribution of adjacent subunits to the active sites of D-3-phosphoglycerate dehydrogenase. *J. Biol. Chem.* **274**, 5357–5361.
18. Schuller, D.J., Grant, G.A. & Banaszak, L.J. (1995) The allosteric ligand site in the Vmax-type cooperative enzyme phosphoglycerate dehydrogenase. *Nat. Struct. Biol.* **2**, 69–76.
19. Grant, G.A., Xu, X.L. & Hu, Z. (1999) The relationship between effector binding and inhibition of activity in D-3-phosphoglycerate dehydrogenase. *Protein Sci.* **8**, 2501–2505.
20. Grant, G.A. & Xu, X.L. (1998) Probing the regulatory domain interface of D-3-phosphoglycerate dehydrogenase with engineered tryptophan residues. *J. Biol. Chem.* **273**, 22389–22394.
21. Klomp, L.W., de Koning, T.J., Malingre, H.E., van Beurden, E.A., Brink, M., Opdam, F.L., Duran, M., Jaeken, J., Pineda, M., Van Maldergem, L., Poll-The, B.T., van den Berg, I.E. & Berger, R. (2000) Molecular characterization of 3-phosphoglycerate dehydrogenase deficiency – a neurometabolic disorder associated with reduced L-serine biosynthesis. *Am. J. Hum. Genet.* **67**, 1389–1399.
22. de Koning, T.J., Duran, M., Dorland, L., Gooskens, R., Van Schaftingen, E., Jaeken, J., Blau, N., Berger, R. & Poll-The, B.T. (1998) Beneficial effects of L-serine and glycine in the management of seizures in 3-phosphoglycerate dehydrogenase deficiency. *Ann. Neurol.* **44**, 261–265.
23. de Koning, T.J., Poll-The, B.T. & Jaeken, J. (1999) Continuing education in neurometabolic disorders – serine deficiency disorders. *Neuropediatrics* **30**, 1–4.
24. WHO PAHO UNESCO Report (1997) A consultation with experts on amebiasis. *Epidemiological Bulletin/PAHO* **18**, 13–14.
25. Tokoro, M., Asai, T., Kobayashi, S., Takeuchi, T. & Nozaki, T. (2003) Identification and characterization of two isoenzymes of methionine γ -lyase from *Entamoeba histolytica*: a key enzyme of sulfur-amino acid degradation in an anaerobic parasitic protist that lacks forward and reverse transsulfuration pathways. *J. Biol. Chem.* **278**, 42717–42727.
26. Nozaki, T., Asai, T., Kobayashi, S., Ikegami, F., Noji, M., Saito, K. & Takeuchi, T. (1998) Molecular cloning and characterization of the genes encoding two isoforms of cysteine synthase in the enteric protozoan parasite *Entamoeba histolytica*. *Mol. Biochem. Parasitol.* **97**, 33–44.
27. Nozaki, T., Asai, T., Sanchez, L.B., Kobayashi, S., Nakazawa, M. & Takeuchi, T. (1999) Characterization of the gene encoding serine acetyltransferase, a regulated enzyme of cysteine biosynthesis from the protist parasites *Entamoeba histolytica* and *Entamoeba dispar*. Regulation and possible function of the cysteine biosynthetic pathway in *Entamoeba*. *J. Biol. Chem.* **274**, 32445–32452.
28. Gillin, F.D. & Diamond, L.S. (1980) Attachment of *Entamoeba histolytica* to glass in a defined maintenance medium: specific requirement for cysteine and ascorbic acid. *J. Protozool.* **27**, 474–478.
29. Gillin, F.D. & Diamond, L.S. (1981) *Entamoeba histolytica* and *Giardia lamblia*: effects of cysteine and oxygen tension on trophozoite attachment to glass and survival in culture media. *Exp. Parasitol.* **52**, 9–17.
30. Ali, V., Shigeta, Y. & Nozaki, T. (2003) Molecular and structural characterization of NADPH-dependent D-glycerate dehydrogenase from the enteric parasitic protist *Entamoeba histolytica*. *Biochem. J.* **375**, 729–736.
31. Ballou, C.E. & Hesse, R. (1956) The synthesis and properties of hydroxypyruvic acid phosphate. *J. Am. Soc.* **78**, 3718–3720.
32. Diamond, L.S., Mattern, C.F. & Bartgis, I.L. (1972) Viruses of *Entamoeba histolytica*. I. Identification of transmissible virus-like agents. *J. Virol.* **9**, 326–341.
33. Diamond, L.S., Harlow, D.R. & Cunnick, C.C. (1978) A new medium for the axenic cultivation of *Entamoeba histolytica* and other *Entamoeba*. *Trans. R. Soc. Trop. Med. Hyg.* **72**, 431–432.
34. Laemmli, U.K. (1970) Cleavage of structural proteins during the assembly of the head of bacteriophage T4. *Nature* **227**, 680–685.
35. Thompson, J.D., Higgins, D.G. & Gibson, T.J. (1994) CLUSTAL W: improving the sensitivity of progressive multiple sequence alignment through sequence weighting, position-specific gap penalties and weight matrix choice. *Nucleic Acids Res.* **22**, 4673–4680.
36. Yang, Z. (1997) PAML: a program package for phylogenetic analysis by maximum likelihood. *Comput. Appl. Biosci.* **13**, 555–556.
37. Felsenstein, J. (2002) PHYLIP (phylogeny inference package). Version 3.6a. Distributed by the Author. University of Washington, Seattle.
38. Page, R.D. (1996) TreeView: an application to display phylogenetic trees on personal computers. *Comput. Appl. Biosci.* **12**, 357–358.
39. Wierenga, R.K., Terpstra, P. & Hol, W.G. (1986) Prediction of the occurrence of the ADP-binding beta alpha beta-fold in proteins, using an amino acid sequence fingerprint. *J. Mol. Biol.* **187**, 101–107.

40. Goldberg, J.D., Yoshida, T. & Brick, P. (1994) Crystal structure of a NAD-dependent D-glycerate dehydrogenase at 2.4 Å resolution. *J. Mol. Biol.* **236**, 1123–1140.
41. Birktoft, J.J. & Banaszak, L.J. (1983) The presence of a histidine-aspartic acid pair in the active site of 2-hydroxyacid dehydrogenases. X-ray refinement of cytoplasmic malate dehydrogenase. *J. Biol. Chem.* **258**, 472–482.
42. Grant, G.A., Hu, Z. & Xu, X.L. (2001) Amino acid residue mutations uncouple cooperative effects in *Escherichia coli* D-3-phosphoglycerate dehydrogenase. *J. Biol. Chem.* **276**, 17844–17850.
43. Field, J., Rosenthal, B. & Samuelson, J. (2000) Early lateral transfer of genes encoding malic enzyme, acetyl-CoA synthetase and alcohol dehydrogenases from anaerobic prokaryotes to *Entamoeba histolytica*. *Mol. Microbiol.* **38**, 446–455.
44. Nixon, J.E., Wang, A., Field, J., Morrison, H.G., McArthur, A.G., Sogin, M.L., Loftus, B.J. & Samuelson, J. (2002) Evidence for lateral transfer of genes encoding ferredoxins, nitroreductases, NADH oxidase, and alcohol dehydrogenase 3 from anaerobic prokaryotes to *Giardia lamblia* and *Entamoeba histolytica*. *Eukaryot. Cell* **1**, 181–190.
45. Zhao, G. & Winkler, M.E. (1996) A novel alpha-ketoglutarate reductase activity of the serA-encoded 3-phosphoglycerate dehydrogenase of *Escherichia coli* K-12 and its possible implications for human 2-hydroxyglutaric aciduria. *J. Bacteriol.* **178**, 232–239.
46. Williamson, D.H., Lund, P. & Krebs, H.A. (1967) The redox state of free nicotinamide-adenine dinucleotide in the cytoplasm and mitochondria of rat liver. *Biochem. J.* **103**, 514–527.
47. Guynn, R.W., Merrill, D.K. & Lund, K. (1986) The reactions of the phosphorylated pathway of l-serine biosynthesis: thermodynamic relationships in rat liver in vivo. *Arch. Biochem. Biophys.* **245**, 204–211.
48. Merrill, D.K., McAlexander, J.C. & Guynn, R.W. (1981) Equilibrium constants under physiological conditions for the reactions of D-3-phosphoglycerate dehydrogenase and l-phosphoserine aminotransferase. *Arch. Biochem. Biophys.* **212**, 717–729.
49. Gardner, M.J., Shallom, S.J., Carlton, J.M., Salzberg, S.L., Nene, V., Shoabi, A., Ciecko, A., Lynn, J., Rizzo, M., Weaver, B., Jarrahi, B., Brenner, M., Parvizi, B., Tallon, L., Moazzez, A., Granger, D., Fujii, C., Hansen, C., Pederson, J., Feldblyum, T., Peterson, J., Suh, B., Angiuoli, S., Pertea, M., Allen, J., Selengut, J., White, O., Cummings, L.M., Smith, H.O., Adams, M.D., Venter, J.C., Carucci, D.J., Hoffman, S.L. & Fraser, C.M. (2002) Sequence of *Plasmodium falciparum* chromosomes 2, 10, 11 and 14. *Nature* **419**, 531–534.
50. Takeuchi, T., Weinbach, E.C., Gottlieb, M. & Diamond, L.S. (1979) Mechanism of l-serine oxidation in *Entamoeba histolytica*. *Comp. Biochem. Physiol. [B]* **62**, 281–285.
51. Hayashi, S., Tanaka, T., Naito, J. & Suda, M. (1975) Dietary and hormonal regulation of serine synthesis in the rat. *J. Biochem. (Tokyo)* **77**, 207–219.
52. Grant, G.A., Xu, X.L. & Hu, Z. (2000) Removal of the tryptophan 139 side chain in *Escherichia coli* D-3-phosphoglycerate dehydrogenase produces a dimeric enzyme without cooperative effects. *Arch. Biochem. Biophys.* **375**, 171–174.
53. Bell, J.K., Pease, P.J., Bell, J.E., Grant, G.A. & Banaszak, L.J. (2002) De-regulation of D-3-phosphoglycerate dehydrogenase by domain removal. *Eur. J. Biochem.* **269**, 4176–4184.

Rab5-associated Vacuoles Play a Unique Role in Phagocytosis of the Enteric Protozoan Parasite *Entamoeba histolytica**

Received for publication, April 4, 2004, and in revised form, August 27, 2004
Published, JBC Papers in Press, September 3, 2004, DOI 10.1074/jbc.M403987200

Yumiko Saito-Nakano†, Tomoyoshi Yasuda‡, Kumiko Nakada-Tsukui†, Matthias Leippe§, and Tomoyoshi Nozaki¶¶

From the †Department of Parasitology, National Institute of Infectious Diseases, 1-23-1 Toyama, Shinjuku-ku, Tokyo 162-8640, Japan, the ‡Zoologisches Institut der Christian-Albrechts-Universität Kiel, Olshausenstrasse 40, 24118 Kiel, Germany, and the §Precursory Research for Embryonic Science and Technology, Japan Science and Technology Agency, 2-20-5 Akebono-cho, Tachikawa, Tokyo 190-0012, Japan

In mammals, Rab5 and Rab7 play a specific and coordinated role in a sequential process during phagosome maturation. Here, we report that Rab5 and Rab7 in the enteric protozoan parasite *Entamoeba histolytica*, EhRab5 and EhRab7A, are involved in steps that are distinct from those known for mammals. EhRab5 and EhRab7A were localized to independent small vesicular structures at steady state. Priming with red blood cells induced the formation of large vacuoles associated with both EhRab5 and EhRab7A ("prephagosomal vacuoles (PPV)") in the amoeba within an incubation period of 5–10 min. PPV emerged *de novo* physically and distinct from phagosomes. PPV were gradually acidified and matured by fusion with lysosomes containing a digestive hydrolase, cysteine proteinase, and a membrane-permeabilizing peptide amoebapore. After EhRab5 dissociated from PPV, 5–10 min later, the EhRab7A-PPV fused with phagosomes, and EhRab7A finally dissociated from the phagosomes. Immunoelectron and light micrographs showed that PPV contained small vesicle-like structures containing fluid-phase markers and amoebapores, which were not evenly distributed within PPV, suggesting that the mechanism was similar to multivesicular body formation in PPV generation. In contrast to Rab5 from other organisms, EhRab5 was involved exclusively in phagocytosis, but not in endocytosis. Overexpression of wild-type EhRab5 enhanced phagocytosis and the transport of amoebapore to phagosomes. Conversely, expression of an EhRab5Q67L GTP form mutant impaired the formation of PPV and phagocytosis. Altogether, we propose that the amoebic Rab5 plays an important role in the formation of unique vacuoles, which is essential

for engulfment of erythrocytes and important for packaging of lysosomal hydrolases, prior to the targeting to phagosomes.

Phagocytosis is a critically important element of host defense against invading pathogens in higher organisms and its molecular mechanism in professional phagocytes, e.g. macrophage, has been extensively studied at the molecular level (1, 2). A number of steps including cell surface binding to ligands and the activation of a signaling pathway leading to F-actin polymerization have been identified as essential for phagocytosis. In addition, membrane trafficking plays an important role in the controlled maturation of phagosomes. The maturation is accompanied by sequential fusion with the endocytic compartment to form a phagolysosome, and is orchestrated by small GTPase, Rab proteins, which act as molecular switches regulating the fusion of vesicles with target membranes through the conformational change between active (GTP-bound) and inactive (GDP-bound) forms (3). It has been reported that Rab5 and Rab7 play an important role in the maturation of phagosomes in macrophages (4).

Rab5 was initially shown to be localized to early endosomes and the plasma membrane, and involved in endocytosis and the endosome fusion (5, 6). Rab5 was also observed on nascent phagosomes, and has been implicated to play an important role in the fusion between phagosomes and early endosomes (7–9). Expression of the GTP form Rab5Q67L mutant or down-regulation of wild-type Rab5 by antisense oligonucleotides perturbed the regulated fusion between phagosomes and endosomes, and resulted in the formation of giant phagosomes in the former case, and reduced activity for killing of ingested bacteria because of the inhibition of phagosome maturation in the latter case (8, 9). In addition to Rab5 *per se*, some of the Rab5 effectors that were implicated in endosome fusion, e.g. EEA1 and phosphatidylinositol 3-kinase (Vps34) (10, 11), also have been identified on the phagosome membrane, suggesting that phosphoinositide metabolism is important for phagosome maturation as seen in the endocytic pathway (12, 13). Rab7 has been implicated in late endosomal membrane trafficking in the endocytic pathway (14), and also in the late stage of phagosome maturation (4, 13). Although a specific role for Rab7 during phagocytosis has not yet been well demonstrated, some intracellular microorganisms have been reported to be capable of blocking the maturation and acidification of phagosomes by interfering with Rab7 (15, 16). It has also been recently demonstrated that a novel effector protein, RILP, is recruited to the phagosomal membrane by Rab7, which promotes fusion between phagosomes and lysosomes (17).

* This work was supported in part by a grant for Precursory Research for Embryonic Science and Technology (PRESTO), Japan Science and Technology Agency, Grant-in-aid for Scientific Research 15790219 (to Y.S.-N.) and 15019120 and 15590978 (to T.N.) from the Ministry of Education, Culture, Sports, Science and Technology of Japan, a grant for Research on Emerging and Re-emerging Infectious Diseases from the Ministry of Health, Labor, and Welfare, a grant for the Project to Promote Development of Anti-AIDS Pharmaceuticals from the Japan Health Sciences Foundation (to T.N.), and a grant from the Deutsche Forschungsgemeinschaft (to M.L.). The costs of publication of this article were defrayed in part by the payment of page charges. This article must therefore be hereby marked "advertisement" in accordance with 18 U.S.C. Section 1734 solely to indicate this fact.

The nucleotide sequence(s) reported in this paper has been submitted to the GenBank™/EBI Data Bank with accession number(s) AB054582 (EhRab5) and AB054583 (EhRab7A).

¶ To whom all correspondence should be addressed: Dept. of Parasitology, National Institute of Infectious Diseases, 1-23-1 Toyama, Shinjuku-ku, Tokyo 162-8640, Japan. Tel.: 81-3-5285-1111 (ext. 2733), Fax: 81-3-5285-1173; E-mail: nozaki@nih.go.jp and nozaki@med.gunma-u.ac.jp.

Besides professional phagocytes from higher eukaryotes, some unicellular organisms such as *Dictyostelium discoideum* and *Entamoeba histolytica* show an inherent ability of phagocytosis. *E. histolytica*, an enteric protozoan parasite that causes an estimated 50 million cases of amebiasis; amebic colitis, dysentery, and extraintestinal abscesses (18), and 40,000–100,000 deaths annually (19), colonizes the human gut and engulfs foreign cells including microorganisms and host cells. Phagocytosis has been implicated to be closely associated with the pathogenesis of the amoeba because phagocytosis-deficient amoeba mutants were shown to be avirulent (20). Although a number of amoebic molecules involved in attachment, phagocytosis, and degradation of microorganisms and host cells have been identified including galactose/*N*-acetylgalactosamine (Gal/GalNAc)-inhibitable lectin (21, 22), cytoskeletal proteins and their associated regulatory molecules (23–25), cysteine proteinases (CP),¹ and pore-forming peptides (*i.e.* amoebapores) (26, 27), the molecular mechanism of phagocytosis in this parasite remains largely unknown.

We presumed that Rab proteins also play an essential and central role in the regulation of phagocytosis and endocytosis in *E. histolytica*. We and other groups (28–31) have reported about 20 *EhRab* genes. An additional 50 putative Rab genes showing significant homology to Rab from other organisms were found in the *E. histolytica* genome data base (data not shown, www.tigr.org). A few *EhRab* proteins have been shown to participate in phagocytosis. *EhRabB* was shown to be located on the plasma membrane and phagocytic mouths in the early phase (up to 5 min) of phagocytosis (29). Putative *EhRab7* and *EhRab11* proteins were reported to be abundant in the endosome fraction labeled with iron-dextran, similar to their putative homologues from mammals (30). To dissect the molecular mechanism of Rab proteins involved in the phagosome biogenesis in *Entamoeba*, we characterized, in the present study, two amebic Rab proteins, *EhRab5* and *EhRab7A*, that show significant homology to mammalian and yeast counterparts. The amoebic Rab5 homologue has several unique characteristics that are dissimilar to those of the mammalian and yeast Rab5. First, *EhRab5* is primarily involved in phagocytosis, not endocytosis. Second, in contrast to mammalian Rab5, which is immediately recruited to phagosomes after the engulfment of bacteria or beads, *EhRab5* is not recruited directly to phagosomes, but colocalizes with *EhRab7A*, forming prephagosomal vacuoles (PPV) prior to fusion with phagosomes. Third, *EhRab5* is required for the formation of PPV and efficient engulfment of red blood cells. Fourth, *EhRab5* plays an important role in the transport of the major membrane-permeabilizing peptide amoebapore. Therefore, in conjunction with *EhRab7A*, *EhRab5* plays a key role in the biogenesis of phagosomes by regulating the formation of PPV and transport of membranolytic and hydrolytic factors during phagocytosis in this parasite.

EXPERIMENTAL PROCEDURES

Organism and Culture—*E. histolytica* trophozoites of HM-1:IMSS cl 6 (32) were cultured axenically in BI-S-33 medium at 35 °C as described previously (33).

Isolation of *EhRab5* and *EhRab7A* cDNAs—A full-length *EhRab5* cDNA was obtained by a degenerate PCR approach, followed by 5'- and 3'-rapid amplification of cDNA ends as previously described (28). A full-length *EhRab7A* gene was obtained by reverse transcriptase-PCR using oligonucleotide primers designed based on sequences previously reported (30, 34). We identified at least eight genes showing significant

homology to Rab7 from other species (data not shown). We designated the *EhRab7* gene showing highest homology to mammalian and yeast Rab7 as *EhRab7A* in the present study and describe the characterization of other *EhRab7* isotypes elsewhere.

Plasmid Constructions to Produce Transgenic Amoeba Lines—*EhRab5* and *EhRab7A* cDNA fragments were amplified by PCR using sense and antisense oligonucleotides containing appropriate restriction sites at the end. Three tandem repeats of hemagglutinin (HA) or c-Myc tags, made of annealed complementary oligonucleotides, were inserted in the engineered *NheI* site, which was located at the fourth or second amino acid codon of *EhRab5* or *EhRab7A* cDNA fragments, respectively (Fig. 1). An expression plasmid, pEhEx, contains the 5'-flanking region cysteine synthase gene (AB000266) containing a putative promoter (35), *BglII* and *XhoI* sites between cysteine synthase 5'- and 3'-flanking regions to insert a gene of interest, cysteine synthase 3'-flanking regions and neomycin resistance gene flanked by the 5' and 3' regions of actin gene, obtained from pA5'A3'NEO (36), for drug selection. The 3HA-*EhRab5* cDNA fragment was inserted into the *BglII*-*XhoI* sites of pEhEx to produce pH5. For construction of a plasmid to co-express *EhRab5* and *EhRab7A* (pH5-M7), a 1.7-kb fragment containing the 3Myc-*EhRab7A* protein-coding region flanked by cysteine synthase 5' and 3' regions was cloned into the *SpeI* site of pH5. *EhRab5*Q67L and *EhRab5*S22N mutants were constructed by PCR-mediated mutagenesis (37). Two *EhRab5* mutants were fused with the 3-HA tag and cloned to pEhEx to produce pH5L or pH5N, respectively. Plasmids to co-express either *EhRab5*Q67L or *EhRab5*S22N and *EhRab7A* were constructed as described above (pH5L-M7 or pH5N-M7, respectively). A plasmid to express green fluorescent protein (GFP)-*EhRab5* fusion protein in amoebae was constructed. GFP was amplified by PCR from GIR222 as a template (38), and cloned into pKT-3M, which contained the cysteine synthase promoter, 3-Myc tag, and *SmaI* and *XhoI* restriction sites to produce pKT-MG. The *EhRab5* protein coding region without the stop codon was ligated into *SmaI*-*XhoI* sites of pKT-MG to produce pKT-GFP5. Detailed information, *e.g.* nucleotide number based on sequences deposited in the data base and positions of inserted restriction sites and 3-HA or 3-Myc epitope, are also shown in Fig. 1B.

Establishment of Epitope-tagged *EhRab*-expressing Amoeba Cell Lines—Wild-type trophozoites were transformed with plasmids by liposome-mediated transfection as previously described (39). Transformants were initially selected in the presence of 3 μ g/ml of Geneticin (Invitrogen). The Geneticin concentration was gradually increased to 6–20 μ g/ml during the following 2 weeks before the transformants were subjected to analyses.

Antibodies—Affinity purified anti-*EhRab5* or anti-*EhRab7A* rabbit antibodies were commercially produced at Oriental Yeasts Co. (Tokyo, Japan) using recombinant amino-terminal glutathione *S*-transferase fusion proteins purified using glutathione-Sepharose 4B (Amersham Biosciences). Anti-HA 16B12 and anti-Myc 9E10 mouse monoclonal antibodies were purchased from Berkeley Antibody Co. (Berkeley, CA). Alexa Fluor anti-mouse and anti-rabbit IgG were obtained from Molecular Probes (Eugene, OR). Anti-amoebic CP2 and human band 3 rabbit antibodies were gifts from Iris Bruchhaus and Egbert Tannich (40), and Yuichi Takakuwa (41), respectively. The production of anti-amoebapore A antibody was previously described (42).

Indirect Immunofluorescence—Amoeba transformants in a logarithmic growth phase were harvested and transferred to 8-mm round wells on glass slides and incubated for 30 min at 35 °C to let trophozoites attach to the glass surface. Gerbil red blood cells were added to each well at 10⁷ cells/ml and incubated for 5–50 min at 35 °C. An indirect immunofluorescence assay was performed as follows. Amoebae were fixed with 3.7% paraformaldehyde in phosphate-buffered saline (PBS) for 10 min at room temperature. Ingested red blood cells were stained with diaminobenzidine (0.84 mM 3,3'-diaminobenzidine, 0.048% H₂O₂, and 50 mM Tris-HCl, pH 9.5) for 5 min (43). Cells were then permeabilized with 0.05% Triton X-100, PBS for 5 min. Samples were reacted with 16B12 (1:1000), 9E10 (1:400), anti-amoebapore A antibody (1:1000), or affinity-purified anti-*EhRab5*, anti-*EhRab7A*, or CP2 antibody (1:200). In most experiments, we used a rabbit antibody raised against recombinant *EhRab5*, amoebapore, and CP, and anti-Myc mouse antibody to detect 3Myc-*EhRab7A* unless mentioned otherwise. The samples were then reacted with Alexa Fluor anti-mouse or anti-rabbit IgG (1:1000). The mouse monoclonal antibodies gave no background signal in the non-transformants because of nonspecific antibody binding under the conditions described above. For the staining of endosomal and lysosomal compartments, amoebae were pulsed with either 2 mg/ml FITC-dextran (Sigma) for 10 min or LysoTracker™ Red DND-99 (Molecular Probes) (1:500) for 12 h at 35 °C. Samples were examined on a

¹ The abbreviations used are: CP, cysteine proteinase; FITC, fluorescein isothiocyanate; PPV, prephagosomal vacuole; GFP, green fluorescent protein; PBS, phosphate-buffered saline; HA, hemagglutinin; *EhRab5*, *Entamoeba histolytica* Rab5; *EhRab7A*, *Entamoeba histolytica* Rab7A.

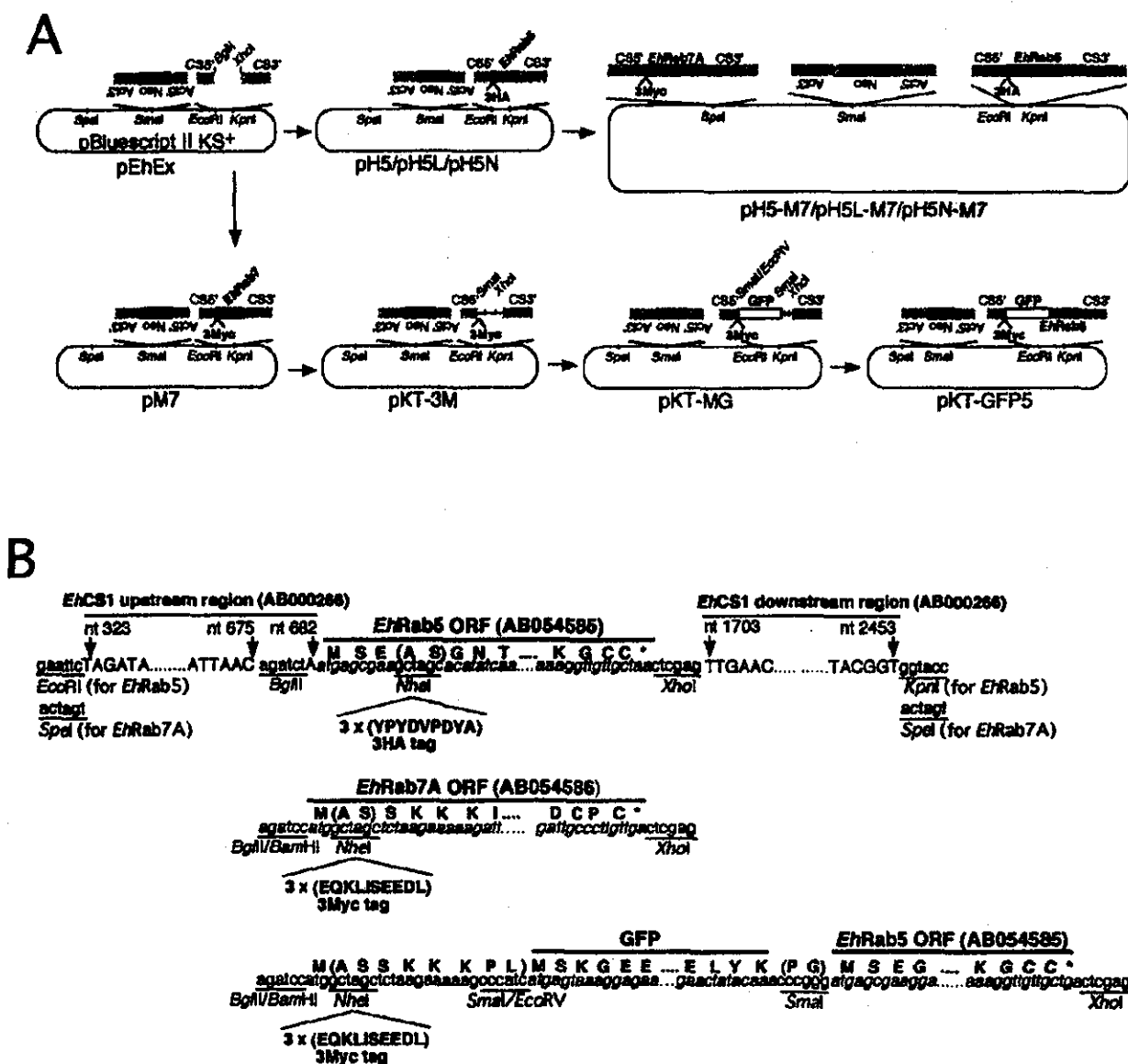


FIG. 1. Plasmids used to express epitope-tagged *EhRab5* and *EhRab7A* in *E. histolytica*. **A**, construction and schematic representation of the plasmids. All plasmids shown are derivatives of pBluescript KS II+. *CS5'*, *CS3'*, *Act5'*, *Act3'*, or *Neo*, 5' upstream or 3' downstream from the cysteine synthase gene, 5' upstream or 3' downstream from the actin gene, or the neomycin resistance gene, respectively. Only representative constructs to express wild-type *EhRab5* and *EhRab7* and GFP are shown. **B**, nucleotide and amino acid sequences of selected regions of the expression cassette for *EhRab5*, *EhRab7A*, and GFP are shown. Nucleotide (nt) number of genes deposited under accession numbers (in parentheses) is shown. Amino acid sequences are shown above nucleotide sequences. (A S), (ASSKKKPL), or (P G) depict inserted amino acids because of engineered restriction sites shown below the nucleotide sequences. An asterisk (*) depicts the stop codon. Restriction sites are underlined. *EhRab5*, *EhRab7A*, and GFP open reading frame are italicized.

Zeiss LSM510 confocal laser-scanning microscope. Images were further analyzed using LSM510 software.

Time-lapse Microscopy—Amoeba transformants expressing GFP-*EhRab5* were plated onto a 35-mm glass-bottom culture dish (D111100, Matsunami Glass Ind. Inc., Osaka, Japan) to settle amoebae at 30°C. After the medium was removed, the glass chamber was enclosed by a glass coverslip. Time-lapse microscopy was performed with a Leica AS MDW system on a Leica DM IRE2 inverted microscope. Images of 18 slices (1.5 μ m apart on the z-axis) were captured at 2.85-s intervals. This z-spacing was optimized to: 1) monitor the entire depth of amoebae from the top to the bottom, and 2) to accomplish fast capturing of a moving amoeba. Obtained raw images were further deconvoluted using Leica Deblur software. For each time point, images were three-dimensionally reconstituted and only a selected plane containing a PPV or a GFP-*EhRab5*-associated compartment was shown.

Immunoelectron Microscopy—Immunoelectron microscopy was per-

formed by pre-embedding labeling method (44). Amoebae were transferred to slide glass and incubated with red blood cells for 10 min as described above. Samples were prefixed with 3.7% paraformaldehyde, PBS for 20 min, and then incubated with 0.1 M glycine, PBS, and permeabilized with 0.1% Triton X-100. Samples were reacted with anti-amoebapore A (1:50), and subsequently with a goat anti-rabbit IgG conjugated with 5-nm gold (1:30). These cells were embedded into 2% soft agar, and further fixed with 0.1% OsO₄, PBS for 30 min followed by dehydration, and embedded in Epon 812 (TAAB Laboratories Equipment LTD., UK). Ultrathin sections were made on an LKB-ultramicrotome (LKB-Produkter, Bromma, Sweden), and sections were stained with uranyl acetate and examined with a Hitachi-H-700 electron microscope.

Measurement of FITC-dextran Uptake—Transformants were cultured in BI-S-33 medium containing 2 mg/ml of FITC-dextran for given periods at 35°C. After the incubation, cells were washed three times

A

```

Eh. Rab5  SEGN-----YDPRKLIQDSGKNSVIVVCFDEYKRF
Hs. Rab5a  STSRSLARPN GQPQASKICRERVITGSAKASSTLRRETCQDFYVGF
Sc. Ypt51  MFSVLS-----LQVILGSAWCKKSSLRRETSNDPRKTKK

Eh. Rab5  NITGSAFLIK TLLVAGELFTEIIRKANDI RNSLHNYV RLSNLIQVY
Hs. Rab5a  SLDGASLIDG SCLLDLITK RITMDAGD RMLR HNYV RASASLQVY
Sc. Ypt51  PLSGASLIDG RITINELNS FEIMDAGD RIFALHNYV RASASLQVY

Eh. Rab5  IISDSEIETG RQIDLRG SGNEAETVVERKQD---DINSVITKEE
Hs. Rab5a  EITKQETIAR APTFKLQR DAPSDVREI ARNNAQL---AKKQKVEYET
Sc. Ypt51  VIKPQLEIK RFDVXILHE DAKDITLAL VGRITMLQE GGEKQIAR

Eh. Rab5  GQVARSLSI DYIETSKAN IYVNEIDOE ARRLTRNKG LIDP-----
Hs. Rab5a  QALADONS EPTETSKTA MANNIDQAE AMILPKSEFQ NLGGS-----
Sc. Ypt51  GQVLEEKG EPTETSKYIG EYVNEVQD GEETLKTAE EQNSSEMER

Eh. Rab5  ---DEIVISN NKNEIKG---  195
Hs. Rab5a  GRSRGLTNE QSQQIKSQE---  215
Sc. Ypt51  SNNQRITNA ANDGISANSA  210
    
```

B

```

Eh. Rab7A  VSKKIKK VITGDSGVC YTSNNDVNR RYGSVYKAT IGAFLITDQL
Hs. Rab7  VITGDSGVC YTSNNDVNR KFGVYKAT IGAFLITDQL
Sc. Ypt7  VNSSEKIKK VITGDSGVC YTSNNDVNR DFGVYKAT IGAFLITDQL

Eh. Rab7A  VYVNHETLV QIINDIANDNEI FQSLGVAFIR GADCCALQVD VNDQVLESL
Hs. Rab7  MVDQLVLYE QIIVTACCEP FQSLGVAFIR GADCCALQVD VYABNEKTLI
Sc. Ypt7  TTEGKLVLYE QIIVTACCEP FQSLGVAFIR GADCCALQVD VYVNSSEKIKK

Eh. Rab7A  NMLFEFLVYQ ASPKNDQDFP FVYEGVYDT YEGSPDAIKR KVEQVQSEHF
Hs. Rab7  DRWFEFLVYQ ASPKNDQDFP FVYEGVYDT YEGSPDAIKR KVEQVQSEHF
Sc. Ypt7  KEWFEFLVYH ANVNSQDFEP FVYEGVYDT YEGSPDAIKR KVEQVQSEHF

Eh. Rab7A  HIPFEFSAK NQINDVDFQ SLSQAMIAK GTEV--DIYV NQVINDQPA
Hs. Rab7  HIPFEFSAK EKINVECAFQ TLRNALKQE TEVELYNEPP EPIKLDKQDQ
Sc. Ypt7  QIIPILFSAK NQINDVDFQ EARSALQCN QAEV--EASE DDYNDAINI

Eh. Rab7A  PQKQSDGSC  206
Hs. Rab7  AKSAECSGSC  208
Sc. Ypt7  LDGENNSGSC  208
    
```

FIG. 2. Comparison of amino acid sequences of Rab5 and Rab7 from *E. histolytica*, human, and yeast. **A**, sequence alignment of *EhRab5*, *Homo sapiens* Rab5a, and *Saccharomyces cerevisiae* Ypt51p. **B**, sequence alignment of *EhRab7A*, *H. sapiens* Rab7, and *S. cerevisiae* Ypt7p. Sequences were aligned by DNASIS (Hitachi Software Engineering Co.). Amino acid residues conserved among at least two species are shown in reverse type. The GTP-binding consensus sequences, the effector region, and the $\alpha 2$ helix are depicted by gray bars, black bars, and double lines, respectively, below the sequences. Computer-generated gaps are shown as dashes.

with 6 ml of ice-cold PBS containing 2% glucose, and solubilized with 50 mM Tris-HCl, pH 7.0, containing 0.1% Nonidet P-40, and 10 μ g/ml of trans-epoxysuccinyl-L-leucylamido-(4-guanidino)butane (E-64). Fluorescence emission at 520 nm was measured with excitation at 490 nm on a fluorescence spectrophotometer (VersaFluor Fluorometer, Bio-Rad) and compared with standards of known concentrations.

RESULTS

Identification of Entamoeba Homologues of Rab5 and Rab7 (*EhRab5* and *EhRab7A*)—We isolated cDNAs coding for a putative homologue of Rab5 and Rab7, and designated them *EhRab5* and *EhRab7A*, respectively. *EhRab5* and *EhRab7A* showed 45 and 48% identity to mammalian Rab5 and Rab7, respectively. The effector region and $\alpha 2$ helix loop, which are important to the specificity of Rab proteins (45), were well conserved among mammals, yeasts, and *E. histolytica* (Fig. 2).

To examine whether the amoebic Rab5 and Rab7A play a role similar to that in other organisms, we attempted to rescue defects of a yeast *Δypt51/Δypt21* mutant (46, 47) and *Δypt7* mutant (14) through ectopic expression of *EhRab5* and *EhRab7A*, respectively. Overexpression of *EhRab5* on a single-copy plasmid under the regulation of a *GAL1* promoter did not complement either the fragmented vacuole morphology or a

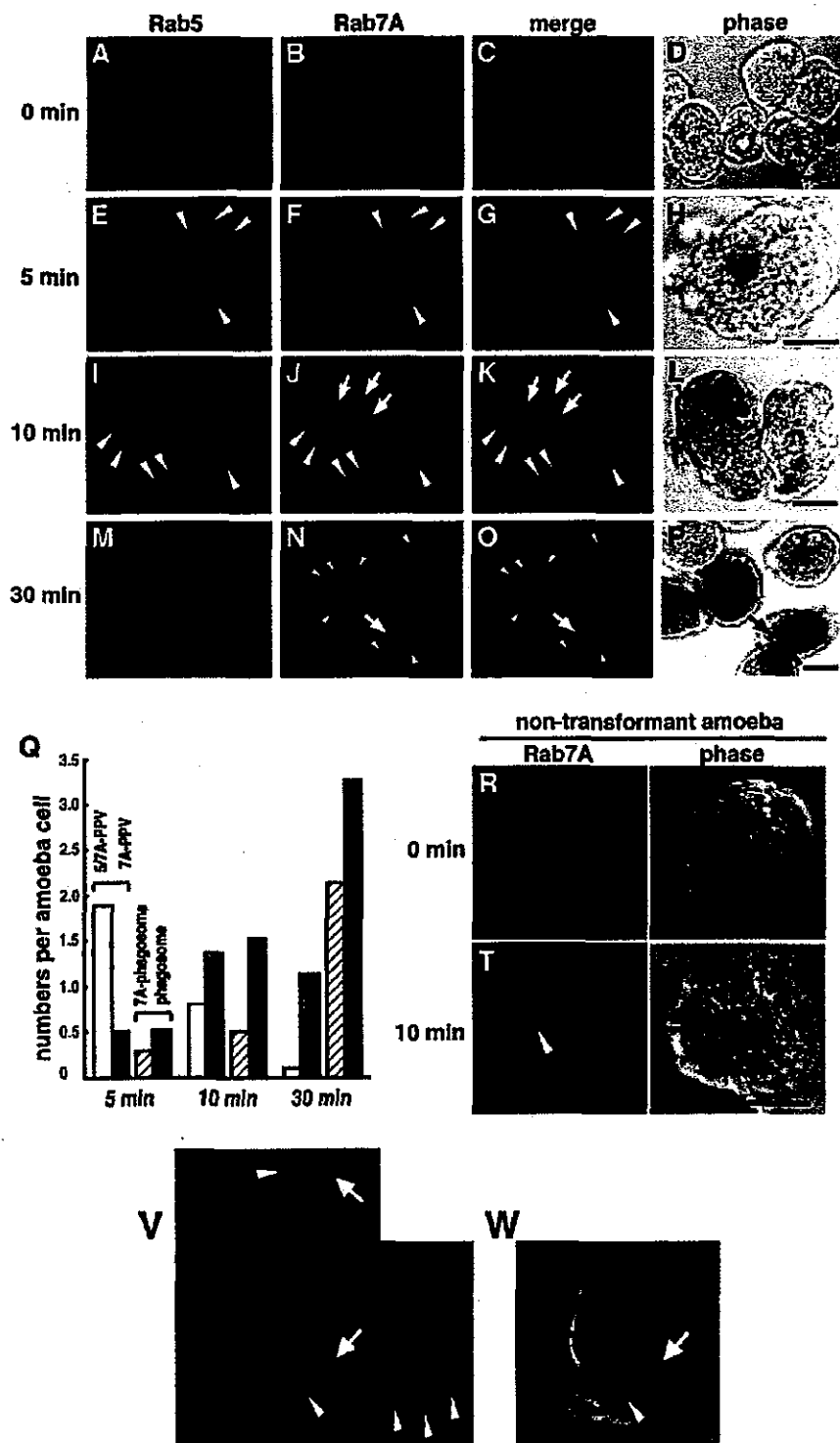
temperature-sensitive growth defect in *Δypt51/Δypt21* cells (data not shown). Neither did overexpression of *EhRab7A* in the *Δypt7* mutant rescue vacuole fragmentation (data not shown). These results indicate that amoebic Rab5 and Rab7A play a role distinct from that of yeast Ypt51p and Ypt7p.

Dynamics of *EhRab5* and *EhRab7A* during Phagocytosis and Identification of Unique PPV Associated with *EhRab5* and *EhRab7A*—We examined the subcellular localization of *EhRab5* and *EhRab7A* during phagocytosis of red blood cells. We constructed a stable transformant that constitutively expressed an 3HA-tagged *EhRab5* and a 3Myc-tagged *EhRab7A*. *EhRab5* and *EhRab7A* were estimated to be overexpressed by 3-5- and 1.5-2-fold, respectively, in the transformant when compared with wild-type cells by quantitation of immunoblots using an antibody raised against recombinant *EhRab5* and *EhRab7A* (data not shown). Neither expression of the epitope-tagged *EhRab5* alone nor co-expression of both epitope-tagged *EhRab5* and *EhRab7A* affected cell growth or morphology (see below and Fig. 8A).

Immunofluorescence imaging using anti-*EhRab5* and anti-Myc antibody, the latter of which reacts with 3Myc-tagged *EhRab7A*, showed that, at steady state (i.e. without red blood cells), *EhRab5* and *EhRab7A* were localized to small non-overlapping vesicles throughout the cytoplasm (Fig. 3, A-D). The distribution of *EhRab5* and *EhRab7A* dramatically changed upon incubation with red blood cells. After 5 min, large vacuoles (4.0 \pm 0.9 μ m in diameter) that colocalized with both *EhRab5* and *EhRab7A* emerged (Fig. 3, E-H). At 10 min, *EhRab5* began to dissociate from some of these vacuoles, whereas *EhRab7A* remained associated with them (Fig. 3, I-L). These *EhRab5/EhRab7A*-positive vacuoles also formed in the amoebae that did not ingest red blood cells (a trophozoite in Fig. 3, E-H, and a trophozoite on the right in Fig. 3, I-L). We designated these vacuoles PPV as this compartment emerged prior to fusion with phagosomes (see below). At 30 min, when the amoebae ingested an average of 3-4 red blood cells per cell, *EhRab5/EhRab7A* double-positive PPV disappeared and *EhRab5* dispersed into the cytosol as seen at steady state. Approximately 40% of phagocytosed red blood cells were surrounded by *EhRab7A* (Fig. 3, N, P, and Q). *EhRab5* was not localized to phagosomes containing red blood cells at any time point (Fig. 3, A, E, I, and M), which is in good contrast to the dynamics shown for mammalian Rab5 in macrophages, where phagosomes are simultaneously associated with both Rab5 and Rab7 (4).

To unequivocally demonstrate the dynamics of the maturation of PPV and phagosomes, we counted (i) *EhRab5/EhRab7A* double-positive PPV, (ii) *EhRab7A* single-positive PPV, (iii) *EhRab7A* positive phagosomes, and (iv) *EhRab7A* negative phagosomes (Fig. 3Q). The number of these vacuoles per cell changed during the course of phagocytosis. The number of *EhRab5/EhRab7A* double-positive PPV peaked at 5 min and gradually decreased after 10 min, whereas the number of *EhRab7A* single-positive PPV increased at 5-10 min, and remained elevated up to 30 min. The proportion of *EhRab5/EhRab7A* double-positive PPV among all PPV (i.e. i/(i + ii)) sharply decreased between 5 and 30 min (78, 37, and 8% at 5, 10, and 30 min, respectively). The number of phagosomes increased linearly during 30 min (0.8 per cell at 5 min to 5.3 per cell at 30 min). However, the proportion of *EhRab7A*-positive phagosomes among all phagosomes (i.e. ii/(iii + iv)) did not significantly change during the course (30-40%). These results support the following model: 1) upon interaction with red blood cells, *EhRab5/EhRab7A* double-positive PPV forms; 2) *EhRab5* is dissociated from *EhRab5/EhRab7A* double-positive PPV; 3)

FIG. 3. Subcellular localization of *EhRab5* and *EhRab7A* changed during red blood cell phagocytosis. *A-P*, subcellular localization of *EhRab5* and *EhRab7A* was examined by immunofluorescence assay using the amoeba transformant co-expressing 3HA-tagged *EhRab5* and 3Myc-tagged *EhRab7A* in the absence of red blood cells (*A-D*), or after 5 (*E-H*), 10 (*I-L*), and 30 min (*M-P*) incubation with red blood cells. Localization of *EhRab5* and *EhRab7A* was examined with anti-*EhRab5* antibody (green; *A, E, I, and M*) and anti-Myc monoclonal antibody (red; *B, F, J, and N*), respectively. Merged images of *EhRab5* and *EhRab7A* (*C, G, K, and O*) and phase-contrast images under transmission light (*D, H, L, and P*) are also shown. Large arrowheads show *EhRab5/EhRab7A*-containing PPV (*E-K*). Small arrowheads (*N-P*) show *EhRab7A*-positive phagosomes. Thick arrows (*J, K, N, O, and P*) indicate *EhRab7A*-PPV, not associated with *EhRab5*. A thin arrow (*L*) indicates an engulfed red blood cell associated with neither *EhRab5* nor *EhRab7A*. *Q*, quantitative analysis of *EhRab5* and *EhRab7A* localization to PPV and phagosomes during erythrophagocytosis. The number of *EhRab5/EhRab7A* double-positive PPV (open bars; also marked as 5/7A-PPV), *EhRab7A* single-positive PPV (gray bars; 7A-PPV), *EhRab7A*-positive phagosomes (hatched bars; 7A-phagosome), and *EhRab7A*-negative phagosomes (filled bars; phagosome) per cell is shown at 5, 10, and 30 min after the addition of red blood cells. *R-U*, subcellular localization of *EhRab7A* was examined by immunofluorescence assay using wild-type amoebae and anti-*EhRab7A* antibody in the absence of red blood cells (*R* and *S*) or after a 10-min (*T* and *U*) incubation with red blood cells. Panels *S* and *U* show phase images of panels *R* and *T*, respectively. Arrowheads in *T* and *U* depict PPV. *V* and *W*, three-dimensional sections of the amoeba containing red blood cell showing the presence of red blood cells in phagosomes, but not in PPV. Localization of PPV and red blood cells was examined with anti-*EhRab5* antibody (green, arrowheads) and anti-band 3 antibody (arrows, red), respectively. Among 17 *z*-sections (1- μ m intervals) obtained with confocal laser scanning microscopy, only one representative *xy* section, together with selected *xz* (green line), and *yz* (red line) sections, are shown. *W* shows a phase image of *V*.



EhRab7A is subsequently targeted to phagosomes; and 4) *EhRab7A* is finally dissociated from phagosomes.

We also verified that PPV was not an artifactually misidentified phagosome, i.e. the phagosome that contains debris of red blood cells, but is not stained by diaminobenzidine because of loss of its content. To exclude this possibility, we used an antibody raised against a major component of the membrane cytoskeleton of red blood cells, band 3 (48). The anti-band 3 antibody clearly reacted with red blood cells in phagosomes

(Fig. 3*V*, red, arrow), whereas none of the *EhRab5*-positive PPV was reacted with the antibody (green, arrowheads). In addition, localization of red blood cells by diaminobenzidine staining or anti-band 3 antibody agreed very well (Fig. 3, *V* and *W*). These results clearly showed that PPV are distinct from phagosomes. The PPV formation was not a secondary defect caused by expression of epitope-tagged *EhRab5* and *EhRab7A* because it was also observed in wild-type amoebae at a comparable frequency, as detected by the antibodies raised against recombi-